Chloride-Responsive Molecular Switch: Driving Ion Transport and Empowering Antibacterial Activities

Sribash Das,[a] Rama Karn,[b] Mohit Kumar,[a] Soumya Srimayee[a] and Debasis Manna*[ab]

[a]Department of Chemistry, Indian Institute of Technology Guwahati, Assam-781039, India.
[b]Centre for Environment, Indian Institute of Technology Guwahati, Assam-781039, India.
Email: dmanna@iitg.ac.in

1. General Information:

The reagents and solvents used in the experiment were purchased from commercial sources such as Sigma-Aldrich and TCI. These were used without undergoing additional purification unless explicitly indicated. The monitoring of reactions was conducted through thin-layer chromatography (TLC) on silica gel 60 F254 (0.25 mm). Silica gel with a mesh size of 120-200 was utilized for the execution of column chromatography. The Bruker spectrometer was used to record the ^{1}H NMR and ^{13}C NMR at 600 MHz and 151 MHz, respectively. The chemical shifts were determined using internal solvents DMSO-d_6 and $CDCl_3$ and were expressed in parts per million (ppm). The values of the coupling constant (J) were expressed in hertz, and the corresponding abbreviations were provided as follows: s (representing singlet), d (representing doublet), t (representing triplet), q (representing quartet), m (representing multiple), and br (representing broadened). High-resolution mass spectra (HRMS) were acquired using an Agilent Q-TOF mass spectrometer equipped with a Z-spray source. The obtained mass data were analyzed using the software integrated into the instrument. The chemical compounds utilized in the study, namely dipalmitoylphosphatidylcholine (DPPC), 1-palmitoyl-2-oleoyl-sn-glycero-3-phospho-L-serine (sodium salt) (POPS) and cholesterol (CHOL), were procured from Sigma Aldrich. The reagents utilized in this study, including HEPES buffer, 8-hydroxylysine-1, 3, 6-trisulfonic acid (HPTS), bis-*N*-methylacridinium nitrate (lucigenin), calcein, Triton X-100, and various inorganic salts, as well as their corresponding hydroxide bases, were procured from Sigma Aldrich. The buffers were prepared using ultrapure water sourced from the Milli-Q system manufactured by Millipore, located in

Billerica, MA. The stock solutions of the compounds were prepared using spectroscopic grade DMSO of gas chromatographic grade, which was procured from Sigma.

2. Synthesis and characterization of compounds:

2.1. Synthesis of 2-(2-aminophenyl)quinazolin-4-amine ─ To the stirring suspension of sodium hydride (178 mg, 7.4 mmol) in THF (10 mL), 2-aminobenzonitril (500 mg, 4.23 mmol) in 10 mL THF was added dropwise under an N_2 atmosphere at 0 °C. After 2 hours, a dropwise solution of 2-aminobenzonitril (500 mg, 4.23 mmol) in dry THF was added and refluxed for an additional 16 hours. After cooling down to room temperature, the reaction mixture was hydrolyzed with an acidic solution (1 equiv HCl in 10 mL of water). After that, the organic solvent was removed under reduced pressure, and 100 mL of water and 20 mL of dichloromethane were added to the resulting residue. The mixture was then neutralized with an aqueous NaOH (1.5 M) solution and three times extracted with 30 mL of dichloromethane. The combined organic layers were dried over sodium sulfate and evaporated to dryness. Then, the crude reaction mixture was purified through column chromatography with a solvent gradient system using ethyl dichloromethane/ MeOH (5%) to furnish the target compound as a yellowish solid (75% yield).[1] The compound was characterized by ^{1}H NMR, ^{13}C NMR, and HRMS (ESI) analysis. **^{1}H NMR (400 MHz, DMSO-*d*$_6$):** δ 9.91-9.88 (m, 4H), 8.50 (d, *J* = 8.2 Hz, 1H), 8.17 (d, *J* = 8.4 Hz, 1H), 8.07 (d, *J* = 8.2 Hz, 1H), 8.00 (t, *J* = 7.6 Hz, 1H), 7.67 (t, *J* = 7.3 Hz, 1H), 7.32 (t, *J* = 7.7 Hz, 1H), 6.92 (d, *J* = 8.4 Hz, 1H), 6.69 (t, *J* = 7.6 Hz, 1H); **^{13}C NMR (151 MHz, DMSO-*d*$_6$):** δ 162.80, 158.59, 151.30, 140.52, 136.55, 134.42, 130.31, 127.55, 125.32, 120.02, 118.22, 115.81, 111.05, 110.67. **HRMS (ESI) *m/z*:** calculated for $C_{14}H_{12}N_4$ $(M + H)^+$: 237.1135, found: 237.1135.

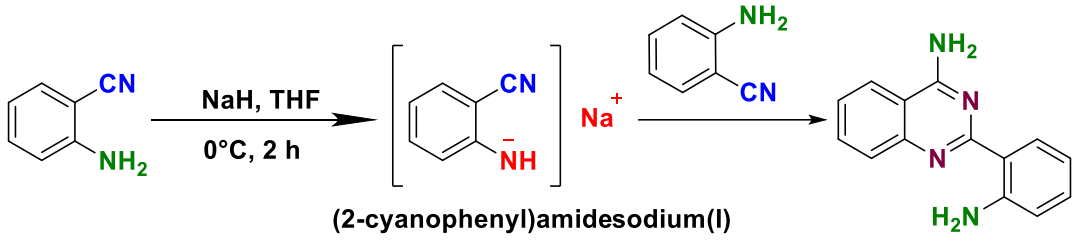

Scheme S1. Synthesis of 2-(2-aminophenyl)quinazolin-4-amine.

2.2. General procedure for the synthesis of thiourea derivatives ─ To the stirring solutions of 2-(2-aminophenyl)quinazolin-4-amine (50 mg, 0.2 mmol, 1 equiv.) and triethylamine (30 µL, 0.2 mmol) in dichloromethane, a solution of respective phenyl isothiocyanate derivatives

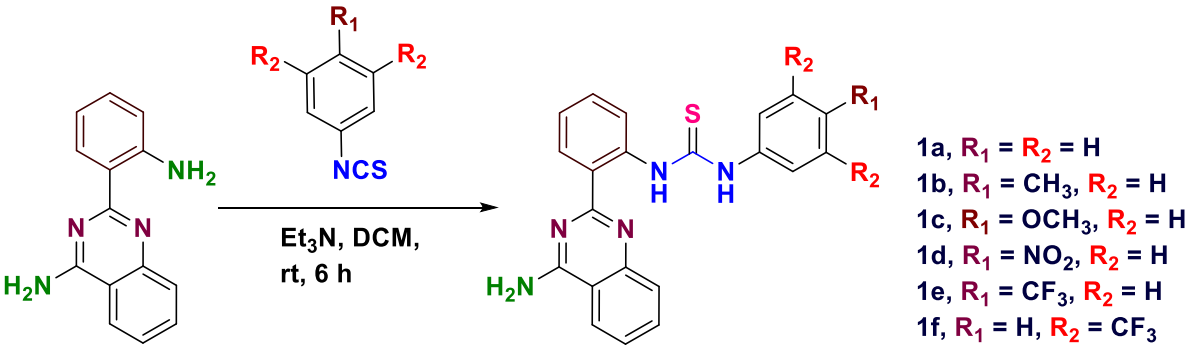

Scheme S2. Synthesis of mono-thiourea derivatives compounds (**1a-1f**).

(0.2 mmol, 1 equiv.) in dichloromethane were added (dropwise) to the reaction mixture under an N_2 atmosphere at room temperature. Then, the reaction mixture was allowed to stir for 6 hours at room temperature. After the completion of the reaction, precipitation happens. The crude precipitate was filtered and washed with dichloromethane and dried at 80 °C overnight, with a resulting yield of 95–98%.[2]

2.3. 1-(2-(4-aminoquinazolin-2-yl)phenyl)-3-phenylthiourea (1a) — The 1-(2-(4-aminoquinazolin-2-yl)phenyl)-3-phenylthiourea (**1a**) was synthesized according to the procedure as mentioned in the earlier section (2.2), using 2-(2-aminophenyl)quinazolin-4-amine (50 mg, 0.21 mmol), phenyl isothiocyanate (30 mg, 0.22 mmol) and triethylamine (30 µL, 0.2 mmol). The yellowish compound was isolated in 95% yield. The compound was characterized by ^{1}H NMR, ^{13}C NMR, and HRMS (ESI) analysis. **^{1}H NMR (600 MHz, DMSO-*d*$_6$):** δ 13.47 (s, 1H), 10.41 (s, 1H), 8.44 (dd, *J* = 13.8, 8.0 Hz, 2H), 8.19 (d, *J* = 8.2 Hz, 1H), 8.11-7.87 (m, 2H), 7.61 (t, *J* = 7.4 Hz, 1H), 7.51 (d, *J* = 7.9 Hz, 2H), 7.46 – 7.45 (m, 4H), 7.26 (t, *J* = 7.3 Hz, 1H), 7.22 (t, *J* = 7.5 Hz, 1H), 6.70 (s, 1H); **^{13}C NMR (151 MHz, DMSO-*d*$_6$):** δ 178.93, 162.20, 160.64, 148.64, 140.43, 139.39, 133.65, 130.44, 129.69, 127.05, 126.50, 126.30, 125.41, 124.92, 124.06, 123.93, 123.45, 112.95. **HRMS (ESI) *m/z*:** calculated for $C_{21}H_{17}N_5S$ $(M + H)^+$: 372.1277, found: 372.1277. **Melting point:** 205 ± 2 °C.

2.4. 1-(2-(4-aminoquinazolin-2-yl)phenyl)-3-(p-tolyl)thiourea (1b) — The 1-(2-(4-aminoquinazolin-2-yl)phenyl)-3-(p-tolyl)thiourea (**1b**) was synthesized according to the procedure as mentioned in the earlier section (2.2), using 2-(2-aminophenyl)quinazolin-4-amine (40 mg, 0.17 mmol), 4-Methylbenzyl isothiocyanate (26 mg, 0.18 mmol) and triethylamine (24 µL, 0.2 mmol). The yellowish compound was isolated in 95% yield. The

compound was characterized by ^{1}H NMR and ^{13}C NMR, and HRMS (ESI) analysis. **^{1}H NMR (600 MHz, $CDCl_3$ + DMSO-d_6):** δ 13.46 (s, 1H), 8.97 (s, 1H), 8.59 (d, *J* = 8.3 Hz, 1H), 8.44 (d, *J* = 7.9 Hz, 1H), 7.97 – 7.92 (m, 1H), 7.54 (t, *J* = 7.5 Hz, 1H), 7.45 (t, *J* = 1.8 Hz, 1H), 7.45 – 7.42 (m, 1H), 7.38 (d, *J* = 3.4 Hz, 2H), 7.36 (d, *J* = 2.4 Hz, 1H), 7.24 (d, *J* = 7.6 Hz, 2H), 7.20 (t, *J* = 7.6 Hz, 1H), 6.79 (s, 1H), 6.48 (s, 2H), 2.40 (s, 3H). **^{13}C NMR (151 MHz, $CDCl_3$ + DMSO-d_6)** δ 178.57, 161.46, 160.25, 148.91, 139.99, 136.17, 134.77, 132.68, 130.20, 129.69, 128.98, 127.16, 126.64, 125.41, 124.30, 123.87, 123.20, 122.96, 112.66, 20.81. **HRMS (ESI) *m/z*:** calculated for $C_{22}H_{19}N_5S$ $(M + H)^+$: 386.1434, found: 386.1438. **Melting point:** 218 ± 2 °C.

2.5. 1-(2-(4-aminoquinazolin-2-yl)phenyl)-3-(4-methoxyphenyl)thiourea (1c) ─ The 1-(2-(4-aminoquinazolin-2-yl)phenyl)-3-(4-methoxyphenyl)thiourea (**1c**) was synthesized according to the procedure as mentioned in the earlier section (2.2), using 2-(2-aminophenyl)quinazolin-4-amine (40 mg, 0.17 mmol), 4-Methoxylbenzyl isothiocyanate (30 mg, 0.18 mmol) and triethylamine (24 µL, 0.2 mmol). The yellowish compound was isolated in 95 % yield. The compound was characterized by ^{1}H NMR, ^{13}C NMR, and HRMS (ESI) analysis. **^{1}H NMR (600 MHz, $CDCl_3$ + DMSO-d_6):** δ 13.09 (s, 1H), 8.56 (s, 1H), 8.45 (d, *J* = 6.5 Hz, 1H), 7.75 (s, 1H), 7.67 (d, *J* = 8.0 Hz, 1H), 7.63 (t, *J* = 7.8 Hz, 1H), 7.51 (t, *J* = 7.7 Hz, 1H), 7.45 (t, *J* = 6.3 Hz, 1H), 7.38 (d, *J* = 8.9 Hz, 2H), 7.27 (m, 4H), 7.00 (d, *J* = 8.9 Hz, 2H), 3.87 (s, 3H). **^{13}C NMR (151 MHz, $CDCl_3$ + DMSO-d_6):** δ 178.87, 161.50, 160.34, 157.17, 148.99, 139.96, 132.70, 131.66, 130.19, 128.92, 127.21, 126.74, 125.74, 125.40, 124.34, 123.28, 122.90, 114.30, 112.68, 55.37. **HRMS (ESI) *m/z*:** calculated for $C_{22}H_{19}N_5OS$ $(M + H)^+$: 402.1382, found: 402.1378. **Melting point:** 192 ± 2 °C.

2.6. 1-(2-(4-aminoquinazolin-2-yl)phenyl)-3-(4-nitrophenyl)thiourea (1d) ─ The 1-(2-(4-aminoquinazolin-2-yl)phenyl)-3-(4-nitrophenyl)thiourea (**1d**) was synthesized according to the procedure as mentioned in the earlier section (2.2), using 2-(2-aminophenyl)quinazolin-4-amine (40 mg, 0.17 mmol), 4-Nitrobenzyl isothiocyanate (30 mg, 0.18 mmol) and triethylamine (24 µL, 0.2 mmol). The orange-coloured solid compound was isolated in 96% yield. The compound was characterized by ^{1}H NMR, ^{13}C NMR, and HRMS (ESI) analysis. ^{1}H NMR (600 MHz, DMSO-d_6) δ 13.99 (s, 1H), 11.02 (s, 1H), 8.51 (m, 8.1 Hz, 2H), 8.24 (t, *J* = 7.6 Hz, 4H), 7.89 (d, *J* = 9.1 Hz, 2H), 7.66 (t, *J* = 7.6 Hz, 1H), 7.50 – 7.45 (m, 2H), 7.27 (t, *J* = 7.5 Hz, 1H), 7.18 (d, *J* = 8.3 Hz, 1H). ^{13}C NMR (151 MHz, $CDCl_3$ + DMSO-d_6): δ 183.59, 166.46, 165.14, 154.00, 150.96, 147.56, 144.32, 137.96, 135.33, 134.27, 131.96, 131.45,

130.54, 129.32, 128.77, 128.51, 128.32, 126.45, 121.52, 117.77. **HRMS (ESI) *m/z*:** calculated for $C_{21}H_{16}N_6O_2S$ $(M + H)^+$: 417.1128, found: 4417.1126. **Melting point:** 208 ± 2 °C.

2.7. 1-(2-(4-aminoquinazolin-2-yl)phenyl)-3-(4-(trifluoromethyl)phenyl)thiourea (1e) ─ The 1-(2-(4-aminoquinazolin-2-yl)phenyl)-3-(4-(trifluoromethyl)phenyl)thiourea (**1e**) was synthesized according to the procedure as mentioned in the earlier section (2.2), using 2-(2-aminophenyl)quinazolin-4-amine (40 mg, 0.17 mmol), 4-(Trifluoromethyl)phenyl isothiocyanate (35 mg, 0.18 mmol) and triethylamine (24 µL, 0.2 mmol). The yellow-coloured solid compound was isolated in 97% yield. The compound was characterized by ^{1}H NMR, ^{13}C NMR, and HRMS (ESI) analysis. **^{1}H NMR (600 MHz, DMSO-*d*$_6$):** δ 13.84 (s, 1H), 10.74 (s, 1H), 8.61 – 8.29 (m, 3H), 8.22 (d, *J* = 8.2 Hz, 1H), 8.18 – 7.97 (m, 8H), 7.81 – 7.73 (m, 4H), 7.58 (t, *J* = 7.6 Hz, 2H), 7.47 (t, *J* = 7.6 Hz, 3H), 7.24 (t, *J* = 7.6 Hz, 1H), 6.78 (d, *J* = 7.9 Hz, 1H). **^{13}C NMR (151 MHz, CDCl$_3$ + DMSO-*d*$_6$):** δ 183.68, 166.36, 165.15, 153.82, 147.37, 144.48, 137.87, 135.32, 135.28, 134.24, 131.83, 131.48, 131.00, 130.52, 128.93, 128.89, 128.45, 128.41, 127.92, 127.88, 127.59, 127.55, 117.58. **HRMS (ESI) *m/z*:** calculated for $C_{22}H_{16}F_3N_5S$ $(M + H)^+$: 440.1151, found: 440.1154. **Melting point:** 176 ± 2 °C.

2.8. 1-(2-(4-aminoquinazolin-2-yl)phenyl)-3-(3,5-bis(trifluoromethyl)phenyl)thiourea (1f) ─ The 1-(2-(4-aminoquinazolin-2-yl)phenyl)-3-(4-(trifluoromethyl)phenyl)thiourea (**1e**) was synthesized according to the procedure as mentioned in the earlier section (2.2), using 2-(2-aminophenyl)quinazolin-4-amine (40 mg, 0.17 mmol), 3,5-Bis(trifluoromethyl)phenyl isothiocyanate (48 mg, 0.18 mmol) and triethylamine (24 µL, 0.2 mmol). The yellow-coloured solid compound was isolated in 97% yield. The compound was characterized by ^{1}H NMR, ^{13}C NMR, and HRMS (ESI) analysis. **^{1}H NMR (600 MHz, DMSO-*d*$_6$) δ:** 13.79 (s, 1H), 10.97 (s, 1H), 8.52 (d, *J* = 7.9 Hz, 1H), 8.44 (d, *J* = 8.2 Hz, 1H), 8.31 (s, 2H), 8.27 (d, *J* = 8.2 Hz, 1H), 8.21-8.08 (br, 2H), 7.83 (s, 1H), 7.74 (t, *J* = 7.6 Hz, 1H), 7.53 (t, *J* = 7.7 Hz, 1H), 7.50 (t, *J* = 7.7 Hz, 1H), 7.46 (d, *J* = 8.2 Hz, 1H), 7.28 (t, *J* = 7.5 Hz, 1H), 5.77 (s, 1H); **^{13}C NMR (151 MHz, DMSO-*d*$_6$):** δ 179.51, 162.23, 160.69, 148.88, 142.04, 139.71, 133.85, 130.94, 130.72, 130.14, 127.14, 126.58, 126.44, 124.56, 124.30, 124.13, 123.99, 123.88, 123.86, 123.83, 123.80, 122.76, 120.95, 117.51, 113.13. **HRMS (ESI) m/z:** calculated for $C_{23}H_{15}F_6N_5S$ $(M + H)^+$: 508.1025, found: 508.1025. **Melting point:** 180 ± 2 °C.

2.9. Synthesis of *N*-(2-(4-aminoquinazolin-2-yl)phenyl)benzamide (2a) ─ To the stirring solutions of 2-(2-aminophenyl)quinazolin-4-amine (50 mg, 0.2 mmol, 1 equiv.) and

triethylamine (30 µL, 0.2 mmol) in dichloromethane, a solution of benzoyl chloride (28.2 mg, 0.2 mmol) in dichloromethane were added (dropwise) to the reaction mixture under an N_2 atmosphere at room temperature. The reaction mixture was allowed to be stirred for 6 hours at room temperature. After the completion of the reaction, precipitation happens. The crude precipitate was filtered and washed with dichloromethane and dried at 80 °C overnight, with a resulting yield of 98%. The compound was characterized by ^{1}H NMR, ^{13}C NMR, and HRMS (ESI) analysis. **^{1}H NMR (600 MHz, $CDCl_3$ + DMSO-*d*$_6$):** δ 8.85 (d, *J* = 8.3 Hz, 1H), 8.71 (d, *J* = 8.0 Hz, 1H), 8.26 (d, *J* = 8.2 Hz, 1H), 8.12 (d, *J* = 7.4 Hz, 2H), 7.76 (d, *J* = 7.5 Hz, 1H), 7.72 (d, *J* = 8.3 Hz, 1H), 7.63 (d, *J* = 7.1 Hz, 2H), 7.59 (t, *J* = 7.4 Hz, 2H), 7.47 (q, *J* = 7.6 Hz, 2H), 7.19 (t, *J* = 7.6 Hz, 1H). **^{13}C NMR (151 MHz, $CDCl_3$ + DMSO-*d*$_6$):** δ 165.65, 161.86, 161.09, 148.54, 139.97, 136.13, 133.22, 131.61, 130.75, 130.70, 128.53, 127.45, 126.22, 125.68, 124.01, 123.83, 122.43, 120.06, 112.97. **HRMS (ESI) *m/z*:** calculated for $C_{21}H_{16}N_4O$ $(M + H)^+$: 341.1397, found: 341.1397. **Melting point:** 165 ± 2 °C.

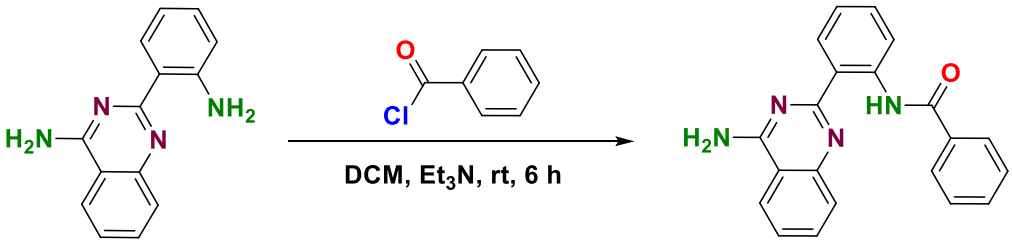

Scheme S3. Synthesis of N-(2-(4-aminoquinazolin-2-yl)phenyl)benzamide.

2.10. Synthesis of *N*-(2-(4-aminoquinazolin-2-yl)phenyl)-4-methylbenzenesulfonamide ─ To the stirring solutions of 2-(2-aminophenyl)quinazolin-4-amine (50 mg, 0.2 mmol, 1 equiv.) and triethylamine (30 µL, 0.2 mmol) in dichloromethane, a solution of benzoyl chloride (40 mg, 0.2 mmol) in dichloromethane were added (dropwise) to the reaction mixture under an N_2 atmosphere at room temperature. The reaction mixture was allowed to be stirred for 6 hours at room temperature. After the completion of the reaction, precipitation happens. The crude precipitate was filtered and washed with dichloromethane and dried at 80 °C overnight, with a resulting yield of 99%. The compound was characterized by ^{1}H NMR, ^{13}C NMR, and HRMS (ESI) analysis. **^{1}H NMR (600 MHz, $CDCl_3$ + DMSO-*d*$_6$)**: δ 8.76 (d, *J* = 8.5 Hz, 1H), 8.01 (s, 1H), 7.85 (d, *J* = 8.2 Hz, 1H), 7.76 – 7.71 (m, 4H), 7.70 – 7.68 (m, 1H), 7.66 – 7.63 (m, 1H), 7.41 – 7.35 (m, 3H), 7.23 (t, *J* = 7.6 Hz, 1H), 7.10 (t, *J* = 7.3 Hz, 1H), 1.73 (s, 8H). **^{13}C NMR (151 MHz, $CDCl_3$ + DMSO-*d*$_6$):** δ 167.44, 162.12, 149.45, 148.42, 143.41, 141.78, 141.59, 141.09, 141.07, 140.85, 140.83, 138.17, 135.23, 134.25, 133.18, 131.38, 130.71, 130.01,

127.10, 116.22, 26.03. **HRMS (ESI) *m/z*:** calculated for $C_{21}H_{18}N_4O_2S$ $(M + H)^+$: 391.1233, found: 391.1219. **Melting point:** 275 ± 2 °C.

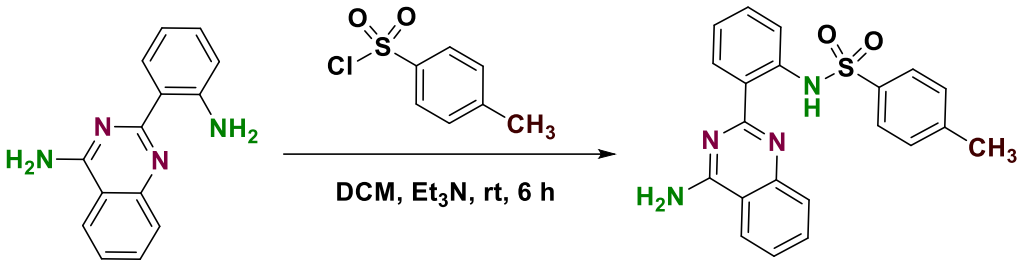

Scheme S4. Synthesis of *N*-(2-(4-aminoquinazolin-2-yl)phenyl)-4methylbenzenesulfonamide.

2.11. Synthesis of bis(thiurea) derivative (3a) — To the stirring solutions of 2-(2-aminophenyl)quinazolin-4-amine (50 mg, 0.2 mmol, 1 equiv.) and triethylamine (30 µL, 0.2 mmol) in DMF, a solution of 1,4 phenylenediisocyanate (22 mg, 0.1 mmol, 0.5 equiv.) in DMF was added dropwise to the reaction mixture under an N_2 atmosphere at room temperature. The reaction mixture was allowed to be stirred for 12 hours at room temperature. After the completion of the reaction, the DMF solvent was removed under reduced pressure. The crude light yellowish solid was washed with dichloromethane and dried at 80 °C overnight, with a yield of 97%. The compound was characterized by ^{1}H NMR, ^{13}C NMR, and HRMS (ESI) analysis. **^{1}H NMR (600 MHz, DMSO-*d*$_6$):** δ 13.45 (s, 2H), 10.55 (s, 2H), 8.44 (t, *J* = 8.6 Hz, 4H), 8.22 (d, *J* = 8.2 Hz, 2H), 8.06 (m, 4H), 7.73 (t, *J* = 7.7 Hz, 2H), 7.61 (s, 4H), 7.47 – 7.44 (m, 4H), 7.23 (t, *J* = 7.6 Hz, 2H), 7.04 (s, 2H). **^{13}C NMR (151 MHz, DMSO-*d*$_6$):** δ 179.01, 162.24, 160.70, 148.75, 140.43, 136.26, 133.93, 130.46, 129.67, 127.29, 126.63, 126.25, 125.04, 124.55, 123.93, 123.43, 112.99. **HRMS (ESI) *m/z*:** calculated for $C_{36}H_{28}N_{10}S_2$ $(M + H)^+$: 665.2013, found: 665.2013. **Melting point:** 188 ± 2 °C.

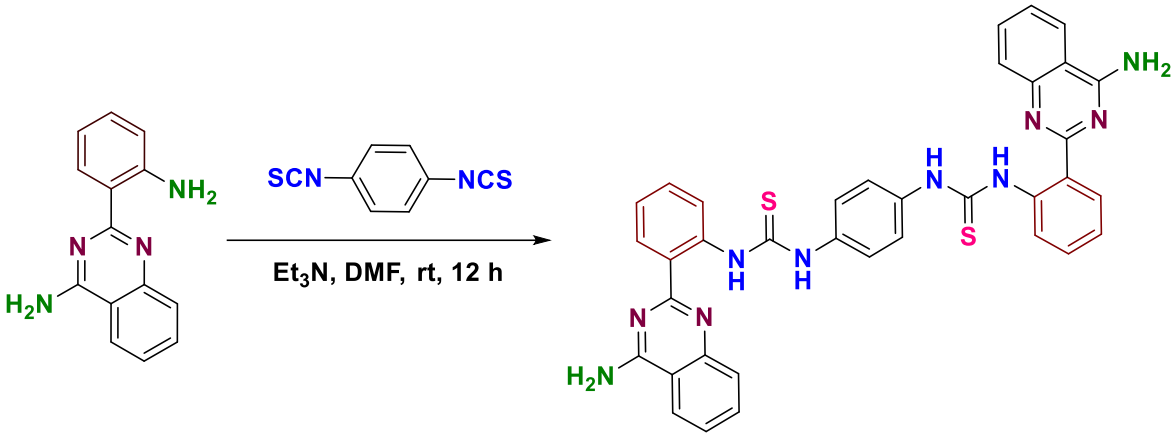

Scheme S5. Synthesis of **3a**.

2.12. Synthesis of bis(thiurea) derivative (3b) — To the stirring solutions of 2-(2-aminophenyl)quinazolin-4-amine (50 mg, 0.2 mmol, 1 equiv.) and triethylamine (30 µL, 0.2 mmol) in DMF, a solution of 1,3-bis(isothiocyanatomethyl)benzene (25 mg, 0.1 mmol, 0.5 equiv.) in DMF was added dropwise to the reaction mixture under an N_2 atmosphere at room temperature. The reaction mixture was stirred for 12 hours at room temperature. After the completion of the reaction, the DMF solvent was removed under reduced pressure. The crude light yellowish solid was washed with dichloromethane and dried at 80 °C overnight, yielding 95 %. The compound was characterized by ^{1}H NMR, ^{13}C NMR, and HRMS (ESI) analysis. **^{1}H NMR (600 MHz, DMSO-*d*$_6$):** δ 12.93 (s, 2H), 9.27 (s, 2H), 8.45 (d, *J* = 8.0 Hz, 2H), 8.27-8.22 (m, 4H), 8.15 – 8.11 (m, 4H), 7.95 (s, 2H), 7.84 (t, *J* = 7.6 Hz, 2H), 7.55 – 7.51 (m, 2H), 7.43 – 7.37 (m, 4H), 7.28 – 7.25 (m, 2H), 7.18 (t, *J* = 7.7 Hz, 2H), 4.83 (d, *J* = 5.8 Hz, 4H). **^{13}C NMR (151 MHz, DMSO-*d*$_6$):** δ 181.65, 162.32, 159.99, 140.30, 139.48, 134.82, 130.61, 128.65, 126.93, 126.79, 126.20, 125.70, 124.53, 123.59, 112.55, 47.45, 45.94. **HRMS (ESI) *m/z*:** calculated for $C_{38}H_{32}N_{10}S_2$ $(M + H)^+$: 693.2326, found: 693.2325. **Melting point:** 180 ± 2 °C.

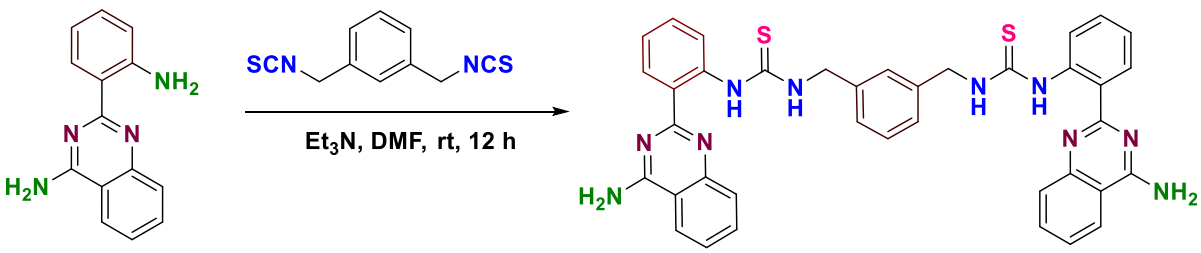

Scheme S6. Synthesis of **3b**.

2.13. Synthesis of 1-(3,5-bis(trifluoromethyl)phenyl)-3-(2-(quinazolin-2-yl)phenyl)thiourea (4) — The compounds 2-(aminomethyl)aniline and 2-(2-nitrophenyl)quinazoline were prepared according to literature procedure [1]. For the synthesis of 2-(quinazolin-2-yl)aniline, to the stirring solutions of 2-(2-nitrophenyl)quinazoline (100 mg, 0.398 mmol, 1 equiv.) and Pd/C (2.2 mg, 0.01 mmol) in EtOH, a solution of hydrazinehydrate (80 %) (100 µL, 1.6 mmol, 4 equiv.) was added dropwise to the reaction mixture under an N_2 atmosphere at room temperature. The reaction mixture was allowed to be stirred for 4 hours at 70 °C temperature. After the completion of the reaction, the mixture was filtered through celite and dried under reduced pressure, with a resulting yellowish-green solid yield of 95–98%. Subsequently, 2-(quinazolin-2-yl)aniline was directly used for the next step. Thereafter, to the stirring solutions of 2-(quinazolin-2-yl)aniline (20 mg, 0.2 mmol, 1 equiv.) in DCM, a solution of 3,5-Bis(trifluoromethyl)phenyl isocyanate (23 mg, 0.09 mmol, 1 equiv.) in DCM was added dropwise to the reaction mixture under an N_2 atmosphere at room temperature. The reaction mixture was allowed to be stirred for 1 hour at room temperature. After the

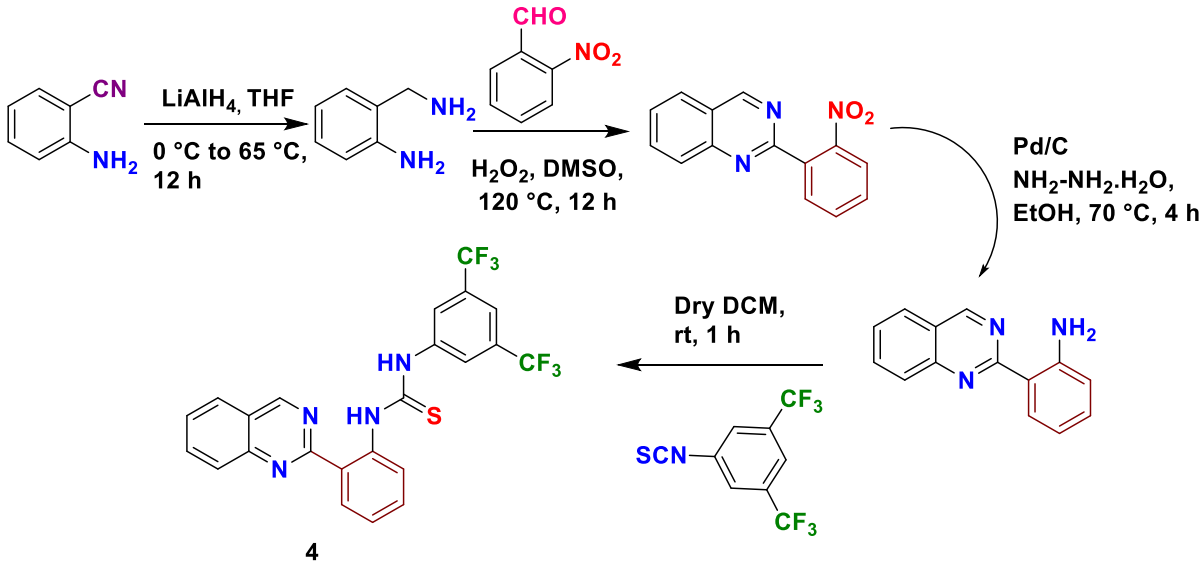

Scheme S7. Synthesis steps for the synthesis of compound **4**.

completion of the reaction, precipitation happens. The crude precipitate was filtered and washed with dichloromethane and dried at 80°C overnight, with a resulting compound **4**, yield of 95–98%. The compounds were characterized by ^{1}H NMR and ^{13}C NMR and HRMS (ESI) analysis. **^{1}H NMR (600 MHz, DMSO-d_6) δ:** 12.30 (s, 1H), 10.94 (s, 1H), 9.74 (s, 1H), 8.48 (d, *J* = 6.6 Hz, 1H), 8.25 (s, 2H), 8.22 (d, *J* = 7.9 Hz, 1H), 8.18 (d, *J* = 8.1 Hz, 1H), 8.04 (t, *J* = 8.2 Hz, 1H), 7.93 (d, *J* = 8.5 Hz, 1H), 7.80 (s, 1H), 7.78 (d, *J* = 7.8 Hz, 1H), 7.56 (t, *J* = 7.7 Hz,

1H), 7.39 (t, *J* = 7.6 Hz, 1H). **^{13}C NMR (151 MHz, DMSO) δ:** 179.96, 161.78, 160.68, 149.11, 142.03, 138.91, 135.67, 131.45, 130.88, 130.81, 130.59, 128.82, 128.41, 127.71, 125.88, 125.22, 124.53, 123.80, 123.12, 122.73. **HRMS (ESI)** ***m/z*:** calculated for $C_{23}H_{14}F_6N_4S$ $(M + H)^+$: 493.0911, found: 493.0911. **Melting point:** 174 ± 2 °C.

2.14. Synthesis of 1-([1,1'-biphenyl]-2-yl)-3-(3,5-bis(trifluoromethyl)phenyl)thiourea (5) — The compound [1,1'-biphenyl]-2-amine was synthesized according to the literature procedure [2]. Thereafter, to the stirring solutions of [1,1'-biphenyl]-2-amine (20 mg, 0.12 mmol, 1 equiv.) in DCM, a solution of 3,5-Bis(trifluoromethyl)phenyl isocyanate (30 mg, 0.12 mmol, 1 equiv.) in DCM was added dropwise to the reaction mixture under an N_2 atmosphere at room temperature. The reaction mixture was allowed to be stirred for 2 hours at room temperature. After the completion of the reaction, precipitation happens. The crude precipitate was filtered and washed with dichloromethane and dried at 80°C overnight, with a resulting compound **5,** yield of 95–98%. The compounds were characterized by ^{1}H NMR, ^{13}C NMR, and HRMS (ESI) analysis. **^{1}H NMR (600 MHz, DMSO-*d*$_6$) δ:** 10.06 (s, 1H), 9.77 (s, 1H), 7.76 (s, 2H), 7.71 (broad, 1H), 7.46 – 7.36 (m, 8H), 7.32 (t, *J* = 7.2 Hz, 1H). **^{13}C NMR (151 MHz, DMSO-*d*$_6$) δ:** 180.78, 142.24, 139.39, 138.78, 135.80, 131.20, 129.02, 128.69, 128.02, 127.68, 124.55, 122.75, 117.32. **HRMS (ESI)** ***m/z*:** calculated for $C_{21}H_{14}F_6N_2S$ $(M + H)^+$: 441.0855, found: 441.0855. **Melting point:** 78 ± 2 °C.

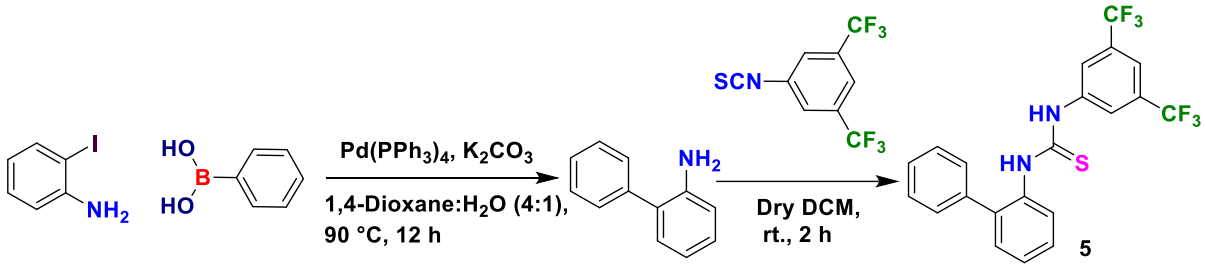

Scheme S8. Synthesis steps for the synthesis of compound **4**.

3. Crystallographic Study:

Using SMART software, the crystallographic data were collected from the Bruker APEX-II CCD diffractometer equipped with a graphite monochromator and Apex CCD camera. All crystallographic data were refined using the SHELXL-2018/3 and or S-20 Olex2 1.2-alpha. Only **1f** was crystalized in an acetonitrile/methanol (1:1) mixture. The tetrabutylammonium

chloride (TBACl) salt was used as a Cl^- source for co-crystallization with the **1f** in DMSO solvent.

Table S1. Crystal parameters and refinement data of the anion complex.

Parameters	**1f**	**1f complexed with Cl^-**
Emperical formula	C23 H15 F6 N5 S	C23 H15 F6 N5 S, C16 H31 N, Cl
Formula weight	507.46	779.32
Temperature (K)	293	293
Crystal system	Monoclinic	Monoclinic
Space group	C2/c	P-21/c
a (A^o)	26.509(6)	9.2259(11)
b (A^o)	8.6693(18)	17.758(2)
c (A^o)	19.550(4)	25.992(3)
α (deg)	90	90
β (deg)	102.969(5)	95.635(4)
γ (deg)	90	90
V (A^{o3})	4378.288	4237.7(9)
Z	8	4
λ	0.71073	0.71073
μ (mm^{-1})	0.222	0.200
Theta (max)	25	2561
h, k, l $_{max}$	31, 10, 23	10, 20, 30
F000	2064	1632
Density (g/cm^{-3})	1.54	1.221
R1, I > 2σ(I	0.1085	0.0879
wR_2	0.1654	0.2113
GooF	1.201	1.076
CCDC	2279459	2279460

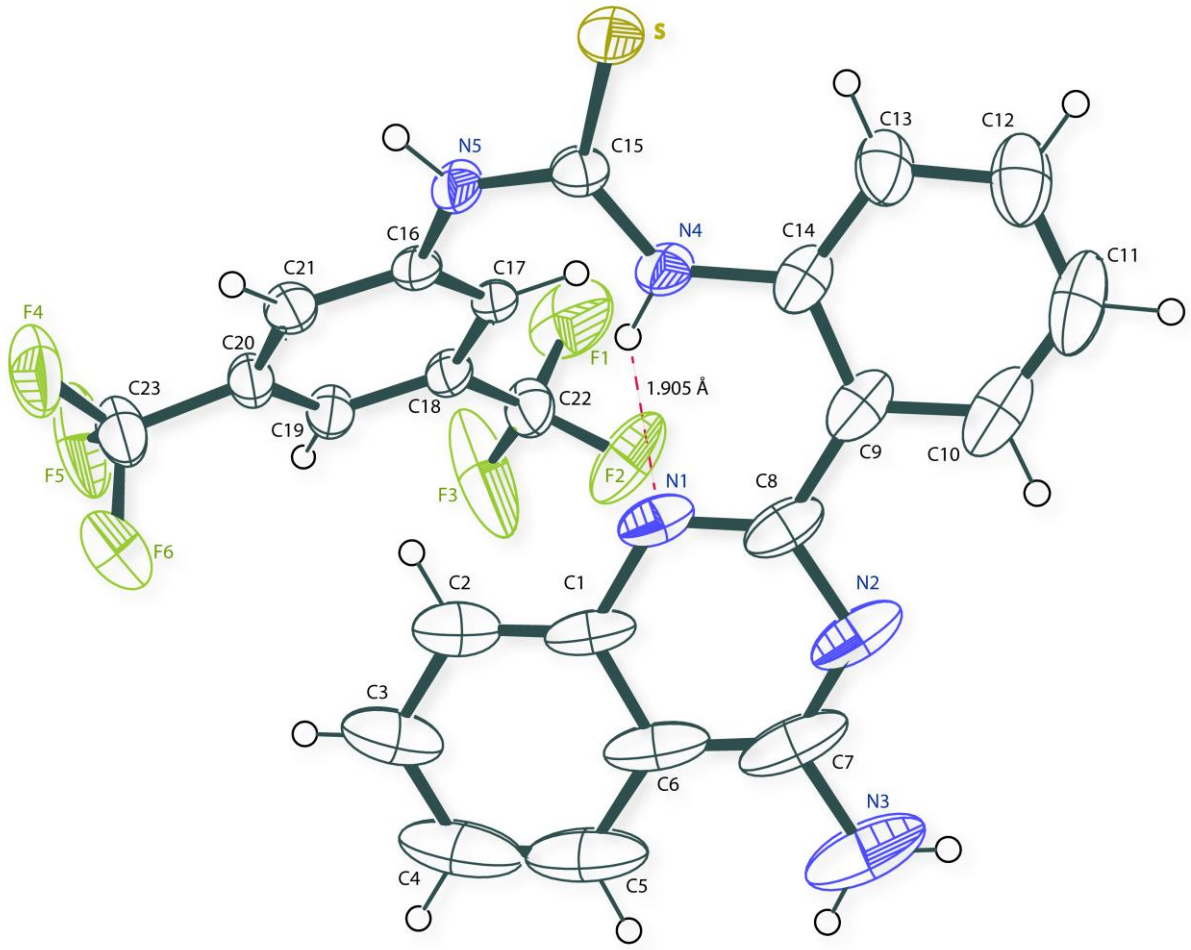

Figure S1. ORTEP diagram of **1f**.

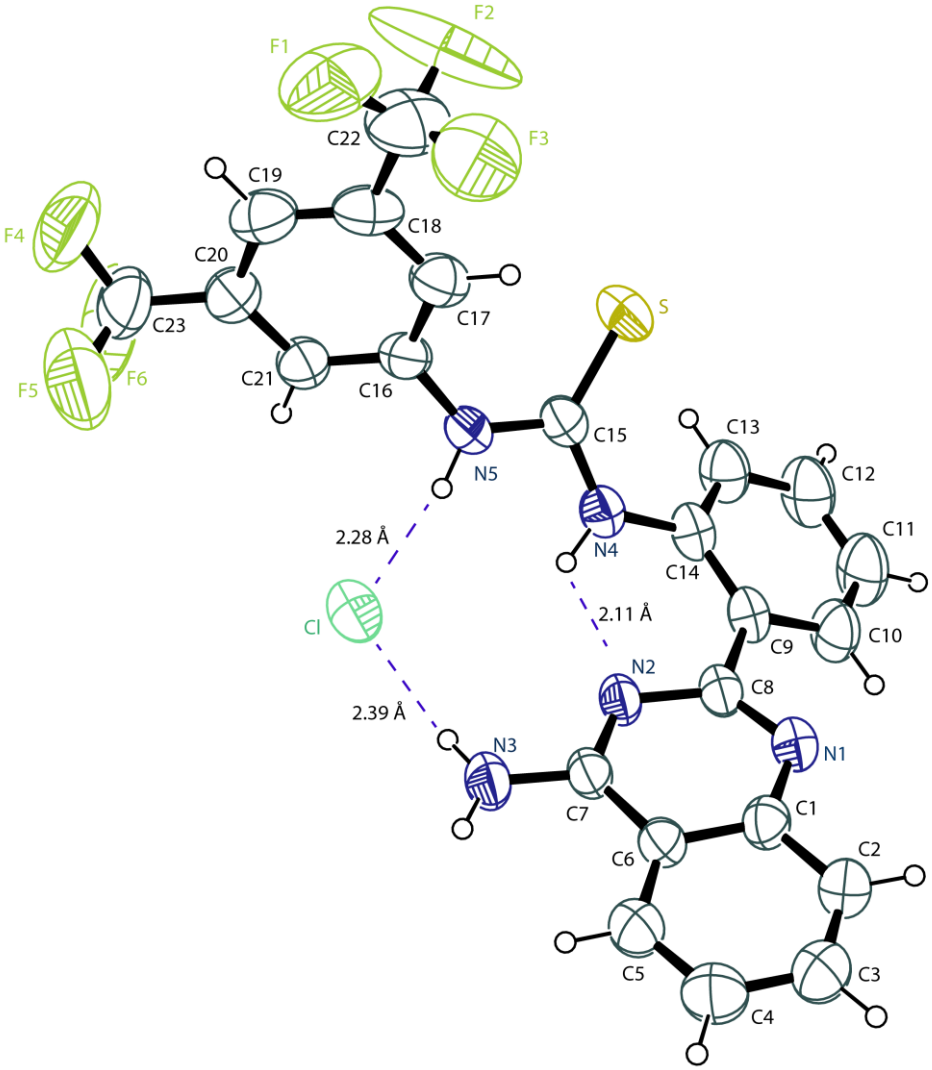

Figure S2. ORTEP diagram of complex **1f** with Cl^-.

4. Anion binding analysis by ^{1}H-NMR titration:

The ^{1}H NMR titration was performed for **1f** in DMSO-d_6. The stock solutions of the compound (10 mM) and TBACl, TBAF, TBABr, TBAI and $TBANO_3$ (1.5 M) were prepared in DMSO-d_6. The tetrabutylammonium or tetraethylammonium salts were used as the source of anions. The ^{1}H NMR titrations of the compound in DMSO-d_6 were performed by the subsequent addition of salt (0-15 equiv.). The changes in chemical shift ($\Delta\delta$) values of the N-H protons of the compounds were analyzed. MestReNova software was used for the stacking of all the titration spectra. The BindFit v0.5 software fitted the changes in a chemical shift against the concentration of anions. The association constant (K_a) values were calculated using the BindFit v0.5 software (1:1 binding model).[2]

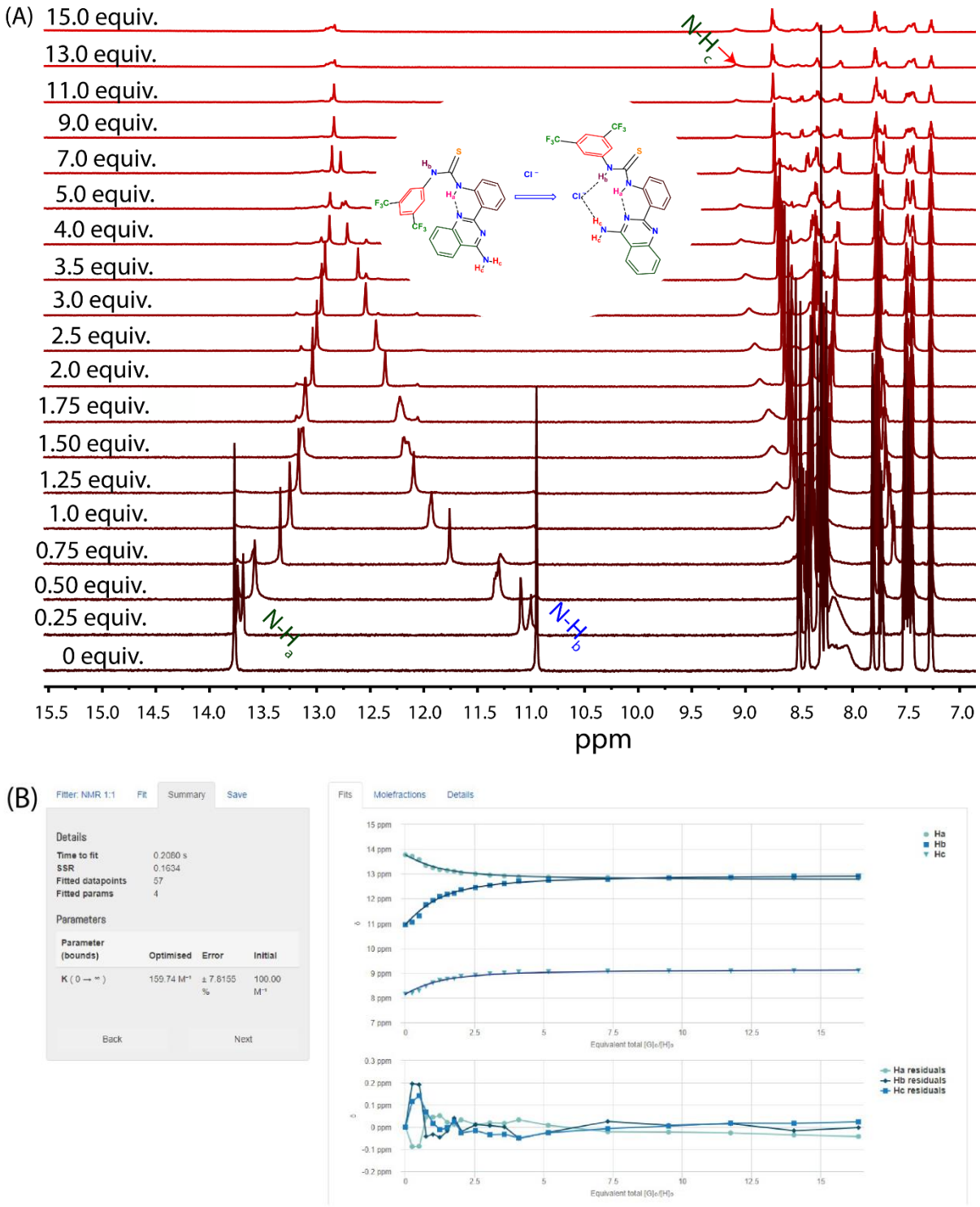

Figure S3. ^{1}H-NMR titration spectra for **1f** (10 mM) with the sequential addition of TBACl in DMSO-d_6 solvent. The amounts of added TBACl are shown on the spectra (**A**). The plot of chemical shift (δ) of N-H_a, N-H_b and N-H_c protons vs. equivalent total ($[G]_0/[H]_0$) added, fitted to 1:1 binding model of BindFit v0.5 program (**B**). H = host = **1f** and G = guest = TBACl.

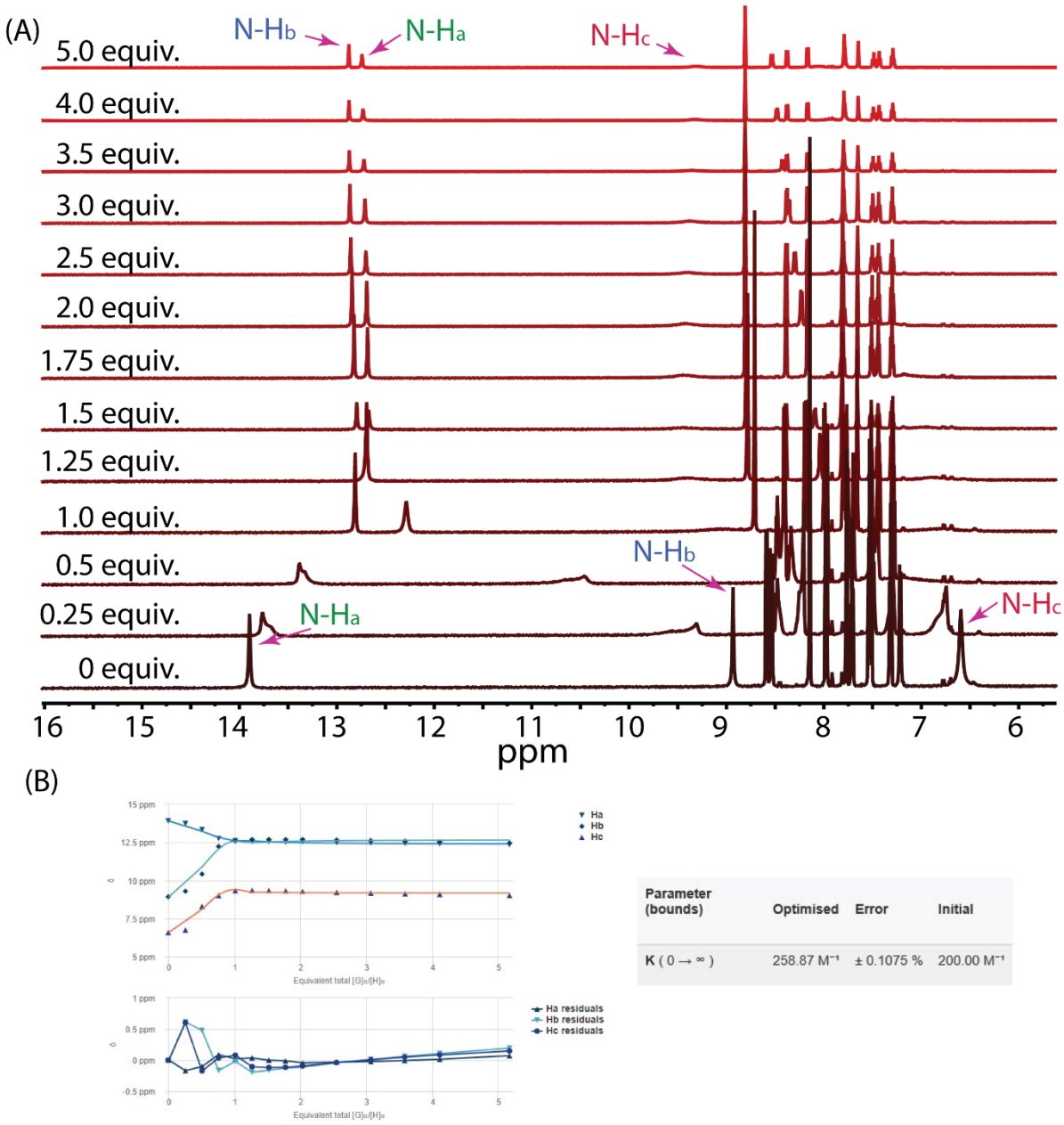

Figure S4. ^{1}H-NMR titration spectra for **1f** (10 mM) with the sequential addition of TBACl in CD_3CN solvent. The amounts of added TBACl are shown on the spectra (**A**). The plot of chemical shift (δ) of N-H_a, N-H_b and N-H_c protons vs. equivalent total ($[G]_0/[H]_0$) added, fitted to 1:1 binding model of BindFit v0.5 program (**B**). H = host = **1f** and G = guest = TBACl.

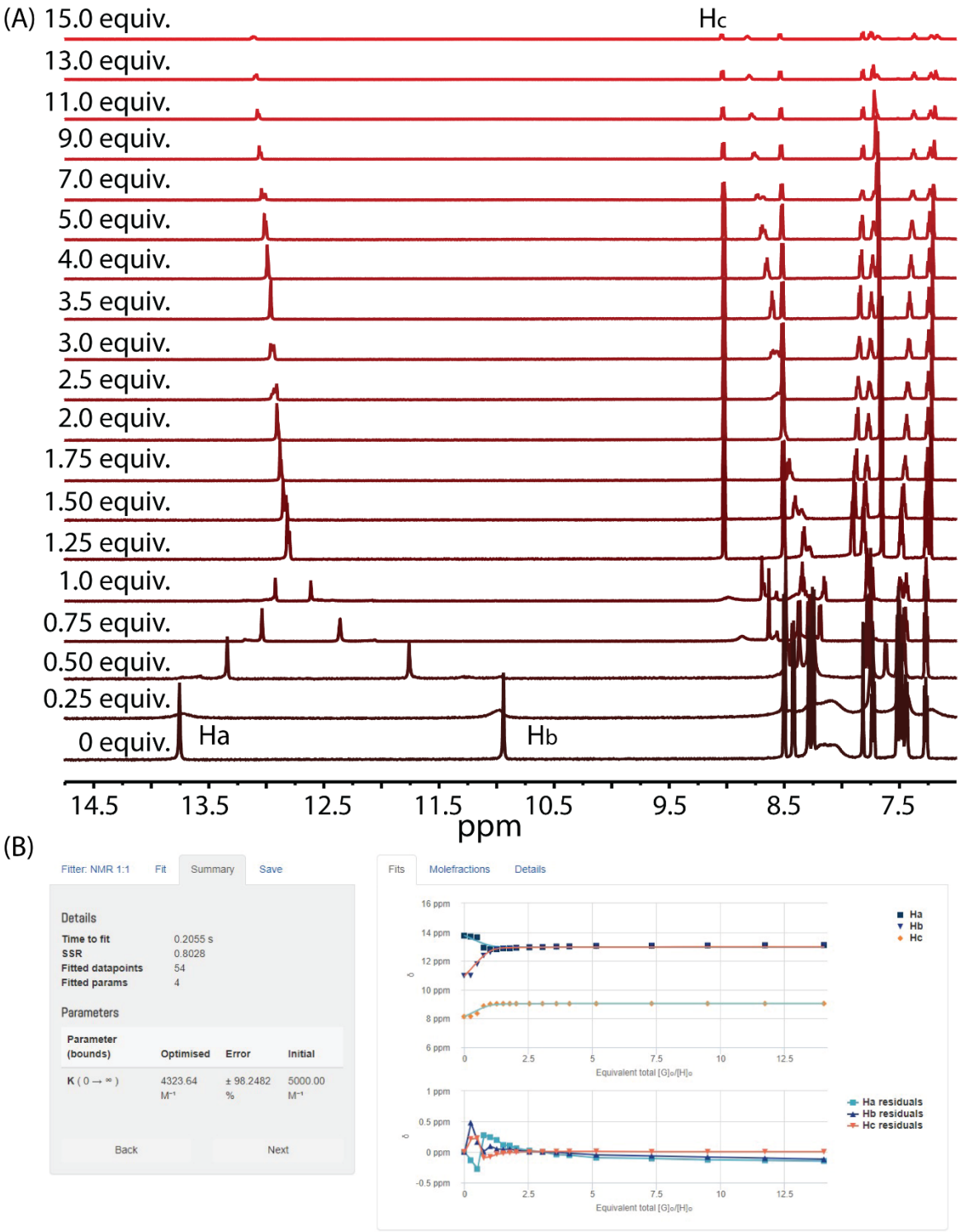

Figure S5. ^{1}H-NMR titration spectra for compound **1f (**10 mM) with the sequential addition of TBAF in DMSO-d_6 solvent. The amounts of added TBAF are shown on the spectra (A). The plot of chemical shift (δ) of N-Ha, N-Hb and N-Hc protons vs. equivalent total ($[G]_0/[H]_0$) added, fitted to 1:1 binding model of BindFit v0.5 program (B). H = host = **1f** and G = guest = TBAF.

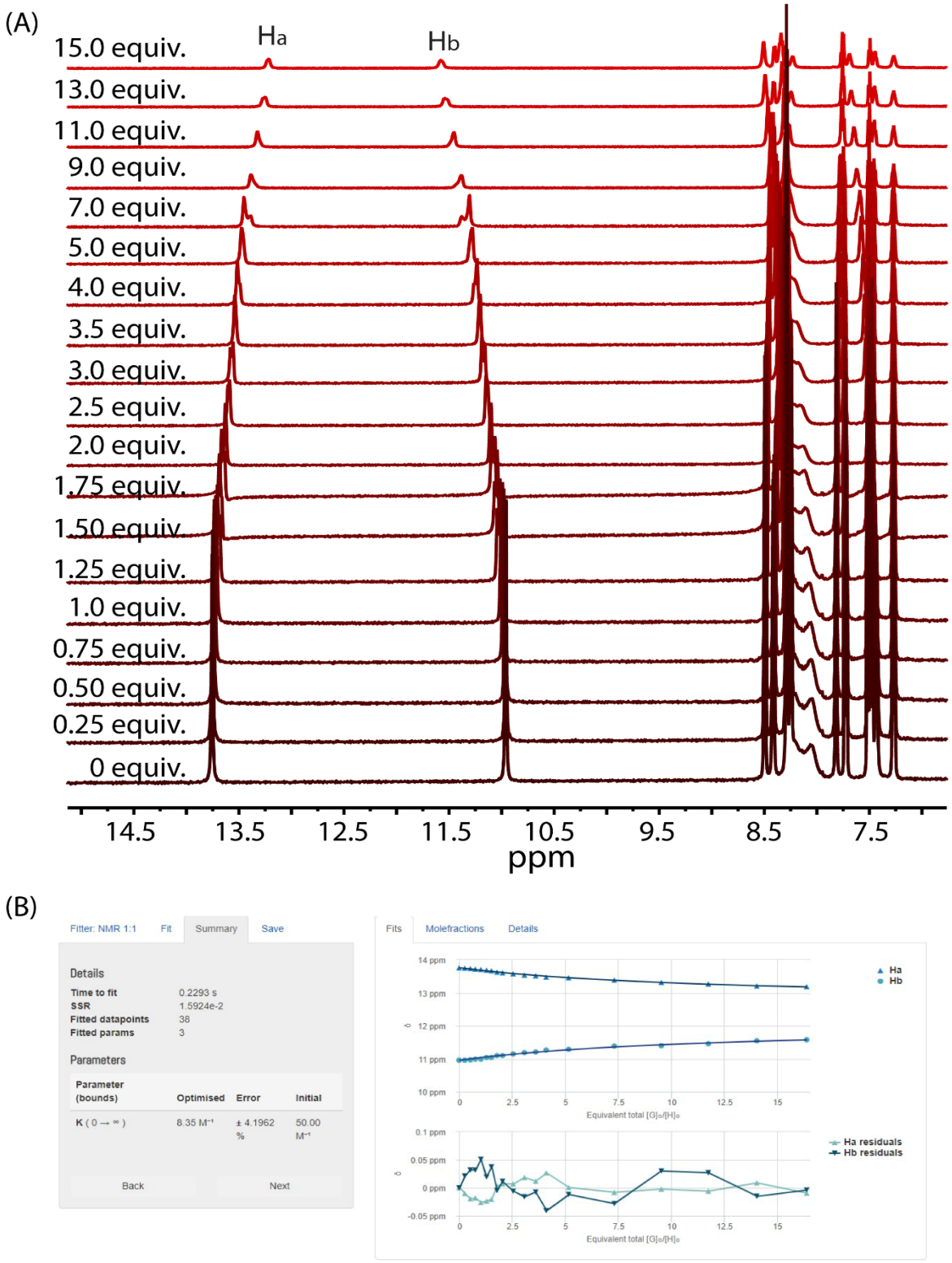

Figure S6. ^{1}H-NMR titration spectra for compound **1f (**10 mM) with the sequential addition of TBABr in DMSO-d_6 solvent. The amounts of added TBABr are shown on the spectra (A). The plot of chemical shift (δ) of N-H_a and N-H_b protons vs. equivalent total ($[G]_0/[H]_0$) added, fitted to 1:1 binding model of BindFit v0.5 program (B). H = host = **1f** and G = guest = TBABr.

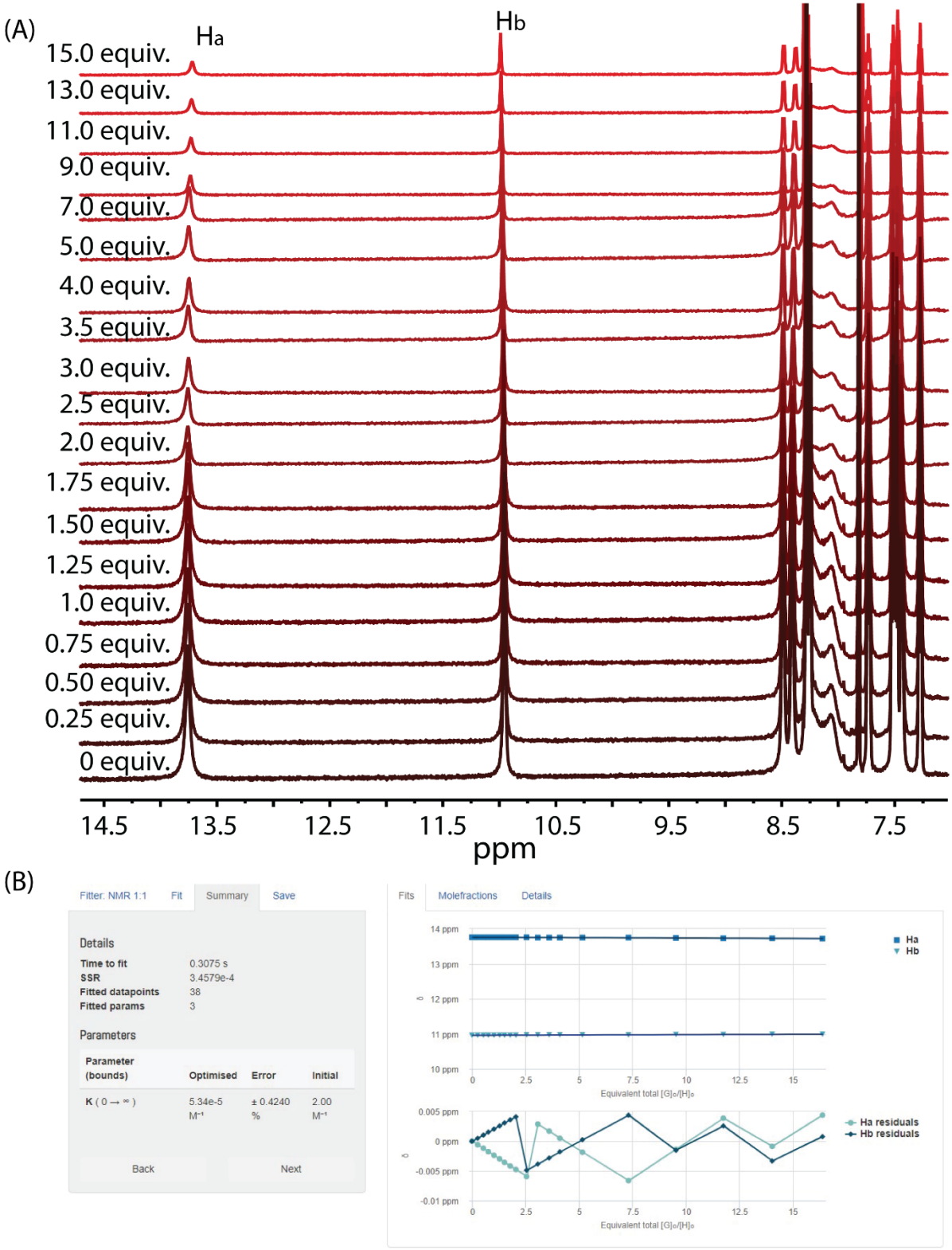

Figure S7. ^{1}H-NMR titration spectra for compound **1f (**10 mM) with the sequential addition of TBAI in DMSO-d_6 solvent. The amounts of added TBAI are shown on the spectra (A). The plot of chemical shift (δ) of N-H_a and N-H_b protons vs. equivalent total ($[G]_0/[H]_0$) added, fitted to 1:1 binding model of BindFit v0.5 program (B). H = host = **1f** and G = guest = TBAI.

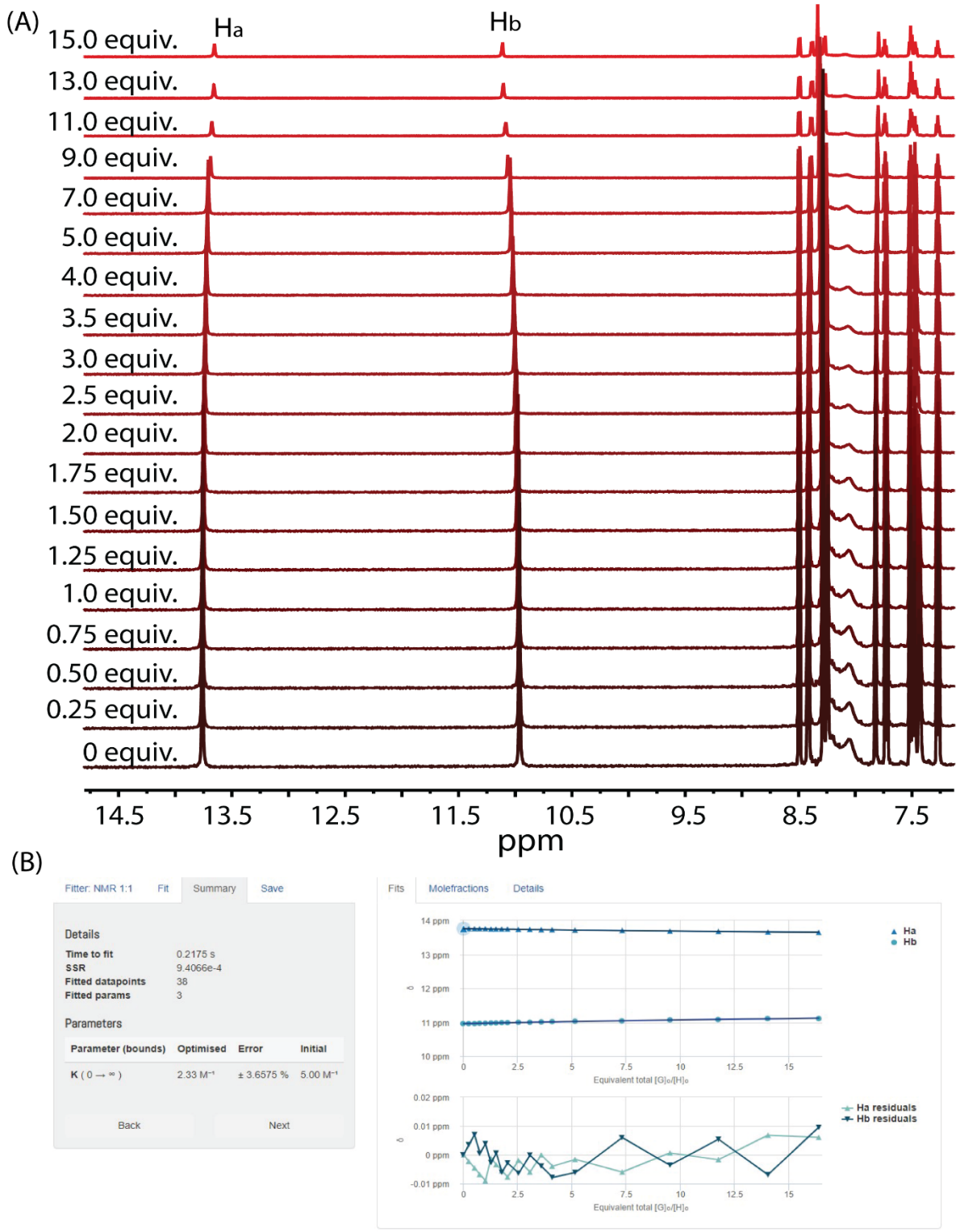

Figure S8. ^{1}H-NMR titration spectra for compound **1f (**10 mM) with the sequential addition of $TBANO_3$ in DMSO-d_6 solvent. The amounts of added $TBANO_3$ are shown on the spectra (A). The plot of chemical shift (δ) of N-H_a and N-H_b protons vs. equivalent total ($[G]_0/[H]_0$) added, fitted to 1:1 binding model of BindFit v0.5 program (B). H = host = **1f** and G = guest = $TBANO_3$.

5. Chloride binding study by using UV-Vis and fluorescence sensing:

To the Quartz fluorescence cuvette (1 mL), **1f** (10 µM) was taken in DMSO solvent. After that, the TBACl solution (stock concentration 1.5 M in DMSO) was added from 0 to 42 mM. In addition, the absorption and emission spectra of **1f** were also recorded.

In a quartz cuvette (2 mL), compound **1f** (10 mM) was taken in spectroscopic DMSO solvent, and different concentrations (from 0 to 42 mM) of tetrabutylammonium chloride (stock concentration 1.5 M in DMSO) were added. All fluorescence measurements were excited at 290 nm and 350 nm. After the saturation point, different amounts of Amberlite IRA-400 resin (1–6 mg) were added to the solution, and fluorescence spectra were taken at the excitation wavelength of 290 nm.

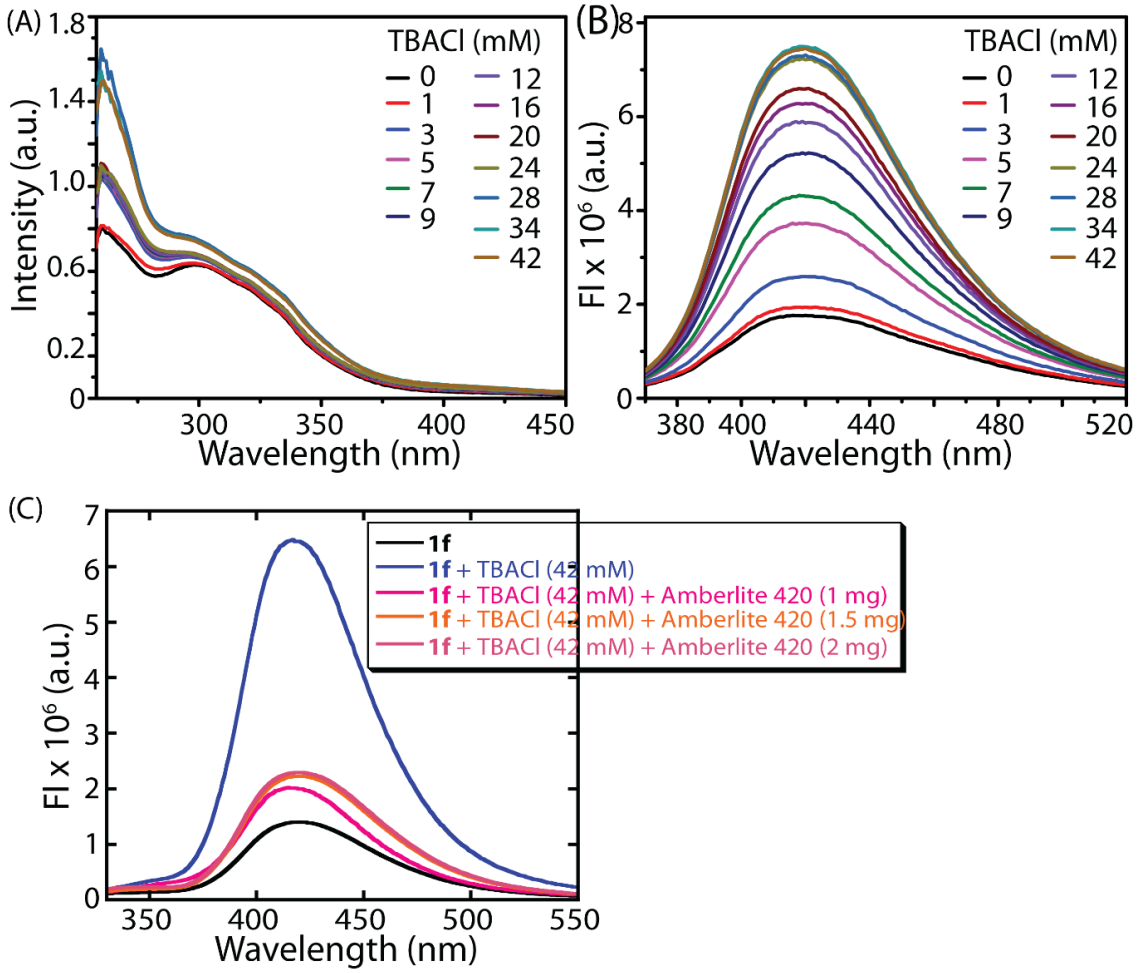

Figure S9. The UV-Vis spectra (A) of **1f** (10 µM) in DMSO solvent. Fluorescence spectra of **1f** with an excitation wavelength of 350 nm (B). The reversibility of Cl^- induced fluorescence enhancement was tested using Amberlite 420 resin (C).

6. Ion transport activity studies:

6.1. Preparation of DPPC/POPS/CHOL-LUVs⊃lucigenin — In order to perform lucigenin-based ion transport studies, DPPC (50 mg/mL in deacidified $CHCl_3$), POPS (50 mg/mL in deacidified $CHCl_3$) and CHOL (25 mg/mL in deacidified $CHCl_3$) was taken in a clean sample vial in the molar ratio of 6:2:2. A thin lipid layer was formed when the fluid was continuously rotated for 6 hours under decreasing pressure. The thin lipid film was hydrated by the addition of 800 µL of 20 mM HEPES buffer containing 1 mM lucigenin and 100 mM $NaNO_3$ solution (pH 7.2 and 5.4). The resulting solution was vortexed 6-7 times for 1 h, subjected to 10-12 freeze-thaw cycles, and then sustained vortexing for 15 minutes to integrate lucigenin into the lipid bilayer. Using a mini-extruder, the lipid suspension was extruded through a polycarbonate membrane from Avanti Polar Lipids with a 200 nm pore size 19-21 times (must be an odd number). To achieve the final lipid content of 25 mM (assume 100% lipid regeneration), the unencapsulated lucigenin dye was removed using size exclusion column chromatography (Sephadex G-50), and a 20 mM HEPES buffer containing 100 mM $NaNO_3$ solution, pH 7.2 as the eluting solution.

6.2. Preparation of DPPC/POPS/CHOL-LUVs⊃HPTS — In order to prepare HPTS encapsulated LUVs, appropriate amounts of DPPC, POPS, and CHOL were combined in a clean, dry glass vial in the molar ratio of 6:2:2. A thin lipid layer was formed when the fluid was continuously rotated for 6 hours under decreasing pressure. The thin lipid film was hydrated by adding 800 µL of 20 mM HEPES, pH 7.2, 100 mM NaCl, and 1 mM HPTS. The resulting solution was vortexed 6-7 times for 1 hour and subjected to 10-12 freeze-thaw cycles. Finally, sustained vortexing for 15 minutes was used to integrate HPTS within the lipid bilayer. Using a mini-extruder, the lipid suspension was extruded through a polycarbonate membrane from Avanti Polar Lipids with a 200 nm pore size 19-21 times (must be an odd number). To achieve the final lipid content of 25 mM (assume 100% lipid regeneration), the free unencapsulated HPTS dye was removed using size exclusion column chromatography (Sephadex G-50) and a 20 mM HEPES buffer containing 100 mM NaCl solution, pH 7.2 as the eluting solution.

6.3. Quantitative measurement of transport activity from lucigenin assay — The fluorescence emission intensities (Y-axis) of the lucigenin dye were normalized, and the intensities appearing at t = 50 and t = 500 s were taken as 0 and 100 units, respectively, and the

normalized fluorescent intensities (FI) at t = 450 s (before the addition of Triton X-100) were considered to measure the transport activity of the compounds.

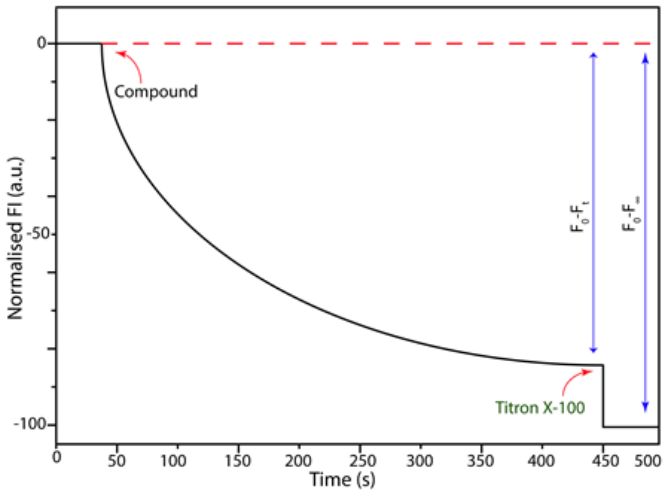

Figure S10. Representations of lucigenin fluorescence-based ion transport kinetics using DPPC/POPS/CHOL-LUVs⊃lucigenin.

The transport activity, $T_{lucigenin} = \frac{F_0 - F_t}{F_0 - F_\infty} \times 100\%$..... Eq. S1

Where, F_0 = fluorescence intensity before the addition of the compound (at t = 45 s), F_∞ = Fluorescence intensity after addition of Triton X-100 (i.e. at saturation, t = 500 s), F_t = Fluorescence intensity at t = 450 s (prior to the addition of Triton X-100).

6.4. Quantitative measurement of transport activity from HPTS assay ─ The fluorescence emission intensities (Y-axis) of the HPTS dye were normalized, and the intensities appearing at t = 50 and t = 500 s were taken as 0 and 100 units, respectively, and the normalized fluorescent intensities (FI) at t = 450 s (prior to the addition of Triton X-100) were considered to measure the transport activity of the compounds.

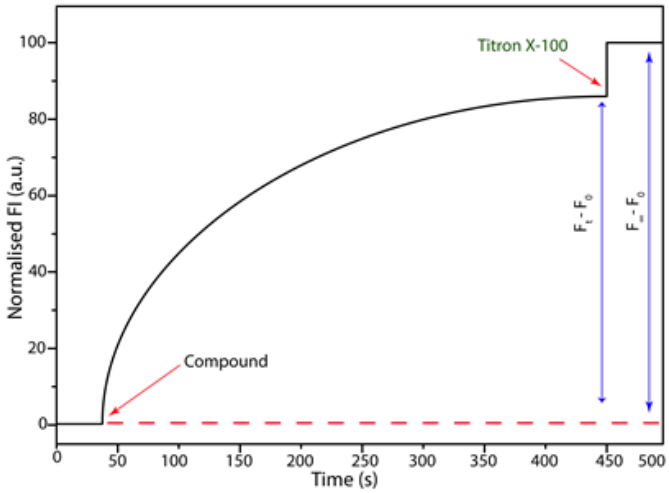

Figure S11. Representation of HPTS-based ion transport kinetics.

The fluorescence intensity was normalized according to Equation S2:

$$T_{HPTS} = \frac{F_t - F_0}{(F_\infty - F_0)} \times 100\ \% \ldots . Eq.S2$$

where, F_0 = Fluorescence intensity just before the compound addition (at t = 50 s). F_∞ = fluorescence intensity at saturation after complete leakage (at t = 450 s). F_t = fluorescence intensity at time t.

6.5. Ion transport activity (lucigenin assay) ─ To perform the lucigenin assay, a 3 mL fluorescence cuvette was filled with 1950 µL of 20 mM HEPES buffer, pH 7.2, containing 100 mM NaCl, and 40 µL of the DPPC/POPS/CHOL-LUVs lucigenin. The cuvette was then placed in the fluorescence spectrophotometer under slow stirring conditions for 3-5 minutes to ensure a homogeneous solution. The kinetic experiment was initiated (at t = 0 s), and the excitation wavelength of lucigenin was 455 nm, with monitoring at 506 nm. After that, the cuvette was maintained in a stirring environment with the chamber temperature set to 25 ^{0}C. Compounds (final concentration 10 µM) were introduced to start the Cl^-inflow kinetics after 45 s. The vesicles were then lysed to end the kinetic experiment. At t = 450 s, the vesicles were finally lysed to end the kinetic experiment by adding 20% Triton X-100 (20 µL) to the cuvette, and fluorescence measurements were conducted for an additional 50 s (t = 500 s).

6.6. pH-dependent Cl^- transport activity across the DPPC/POPS/CHOL-LUVs⊃lucigenin ─ The vesicles were prepared following a similar procedure as the abovementioned method.

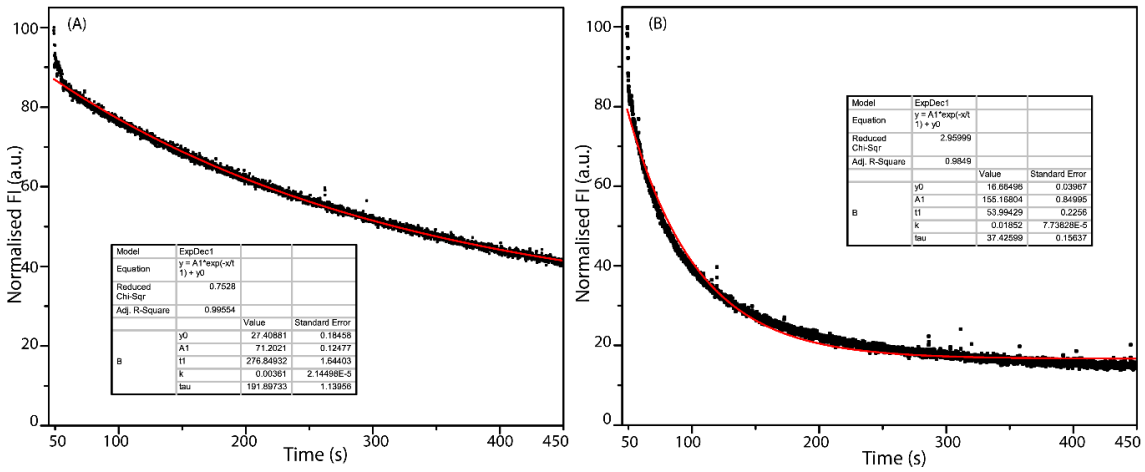

Figure S12. Normalized fluorescence quenching curves (F/F_0) were fitted to a first-order exponential decay equation.

6.7. Concentration-dependent lucigenin assay ─ Similar to the procedure mentioned above, the DPPC/POPS/CHOL-LUVs⊃lucigenin (pH 7.2 and 5.4) was created. The lucigenin dye's fluorescence signals (Y-axis) were scaled from 0 to 100 units [t = 50 to t = 500 s (X-axis)]. The transport activity of **1f** was determined using the normalized fluorescence intensity (FI) values obtained at t = 450 s (before the addition of Triton X-100). Using the earlier Eq.-S1, the transport activity (T) of chemical **1f** at a certain concentration was calculated. The transport activity values (Y-axis) were plotted versus concentration (X-axis) and fitted in the Hill equation to obtain the effective concentration (EC_{50}).[2]

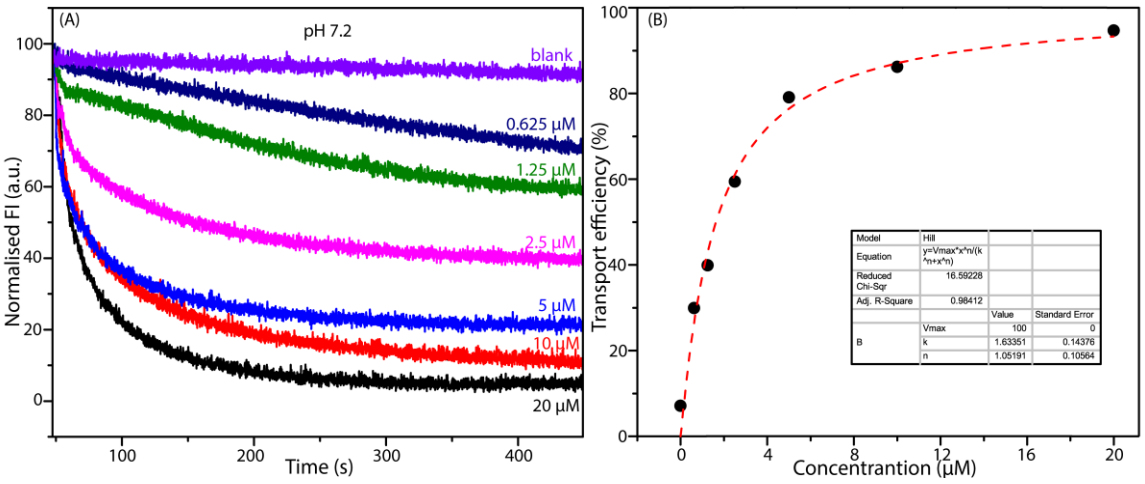

Figure S13. Concentration-dependent transmembrane transport of Cl^- in the presence of **1f** across the DPPC/POPS/CHOL-LUVs⊃lucigenin. The ion transport activity was measured by lucigenin fluorescence assay at pH 7.2. The EC_{50} value was calculated using the Hill equation (B). The compound concentration was varied from 20 to 0.625 µM.

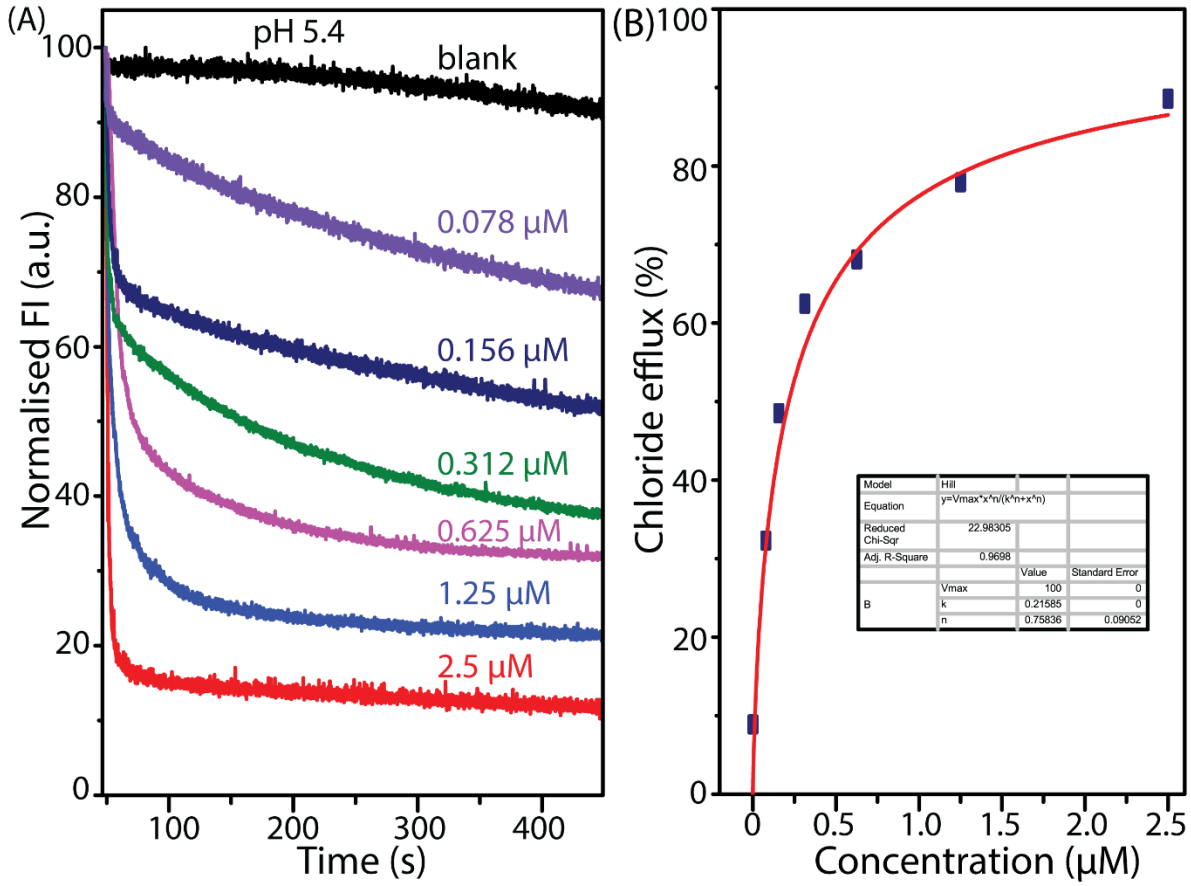

Figure S14. Concentration-dependent transmembrane transport of Cl^- ion in the presence of compound **1f** across the DPPC/POPS/CHOL-LUVs⊃lucigenin. The ion transport activity was measured by lucigenin fluorescence assay at pH 5.4. The EC_{50} value was calculated using the Hill equation (B). The compound concentration was varied from 2.5 to 0.078 μM.

6.8. Chloride transport activity of compound 1f, 4 and 5 across DPPC/POPS/CHOL-LUVs⊃lucigenin ─

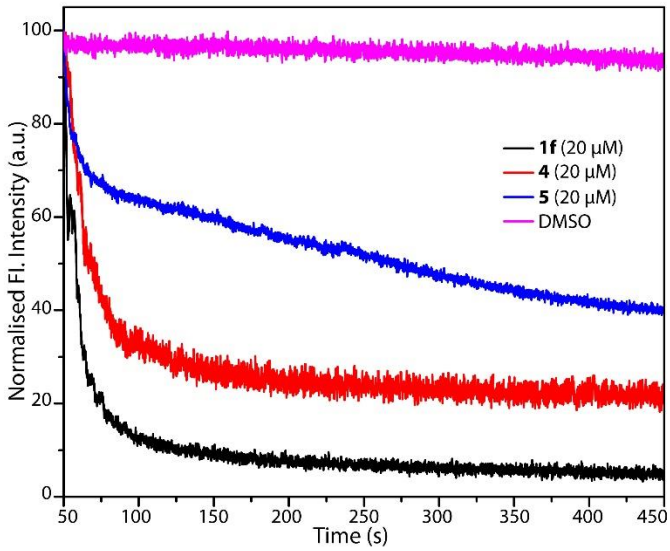

Figure S15. Cl^- transport activity of compound **1f**, **4** and **5 (**20 μM**)** across DPPC/POPS/CHOL-LUVs⊃lucigenin.

6.9. Concentration-dependent lucigenin assay of the compound 4 ─ Similar to the aforementioned procedure, the DPPC/POPS/CHOL-LUVs⊃lucigenin (pH 7.2) was prepared. The lucigenin dye's fluorescence signals (Y-axis) were scaled from 0 to 100 units [t = 50 to t = 500 s (X-axis)]. The transport activity of the compounds was determined using the normalized fluorescence intensity (FI) values obtained at t = 450 s (before the addition of Triton X-100). Using the earlier Eq.-S1, the transport activity (T) of compound **4** at a certain concentration was calculated. The transport activity in % (Y-axis) was plotted against concentration (X-axis) and fitted in the Hill 1 equation to obtain the effective concentration (EC_{50}) of compound **4**.

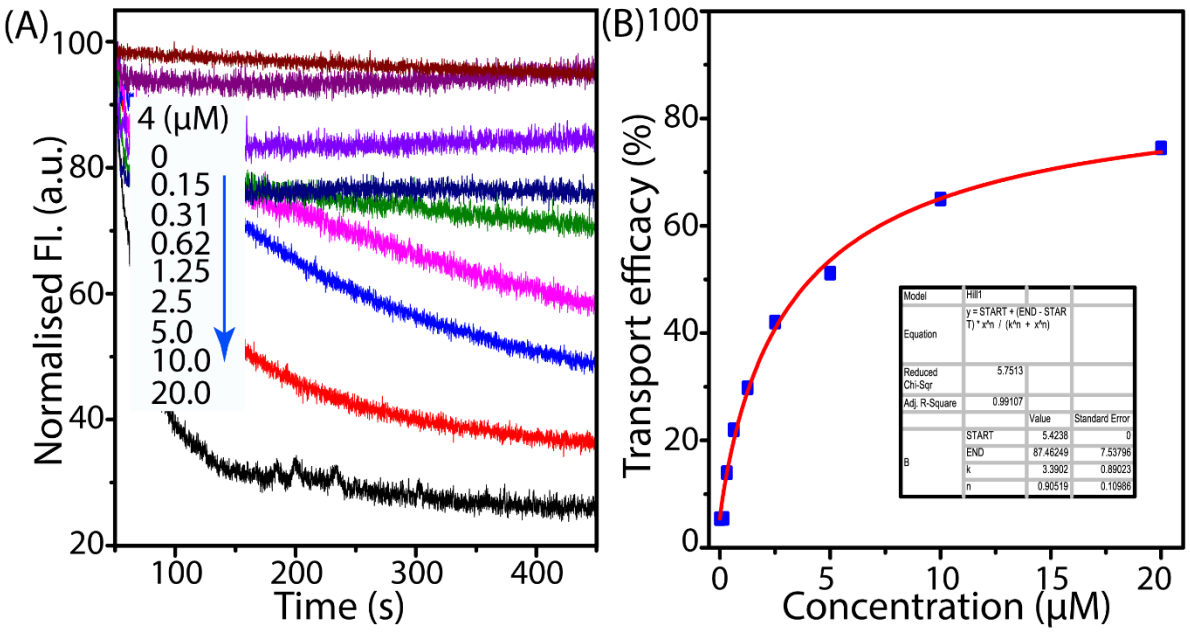

Figure S16. Concentration-dependent transmembrane transport of Cl^- ion in the presence of compound **4** across the DPPC/POPS/CHOL-LUVs⊃lucigenin (A). The ion transport activity was measured by lucigenin fluorescence assay at pH 7.2. The EC_{50} value was calculated using the Hill 1 equation (B). The compound concentration was varied from 20 to 0.15 μM. The EC_{50} of compound found 3.39 ± 0.89 μM.

6.10. Efflux study using chloride ion-selective-electrode (Cl-ISE) ─ Cl-ISE was used to assess the Cl^- efflux efficiency of the compound. Using 20 mM HEPES buffer with 100 mM NaCl and a different pH (pH 7.2), the DPPC/POPS/CHOL-LUVs were made in a manner similar to that described in the section above. The LUVs were first dialyzed against 100 mM $NaNO_3$ in 20 mM HEPES buffer at a pH of 7.2 (iso-osmolar with the NaCl buffer). The Cl^- efflux efficiency of **1f** was assessed using the equation mentioned above.

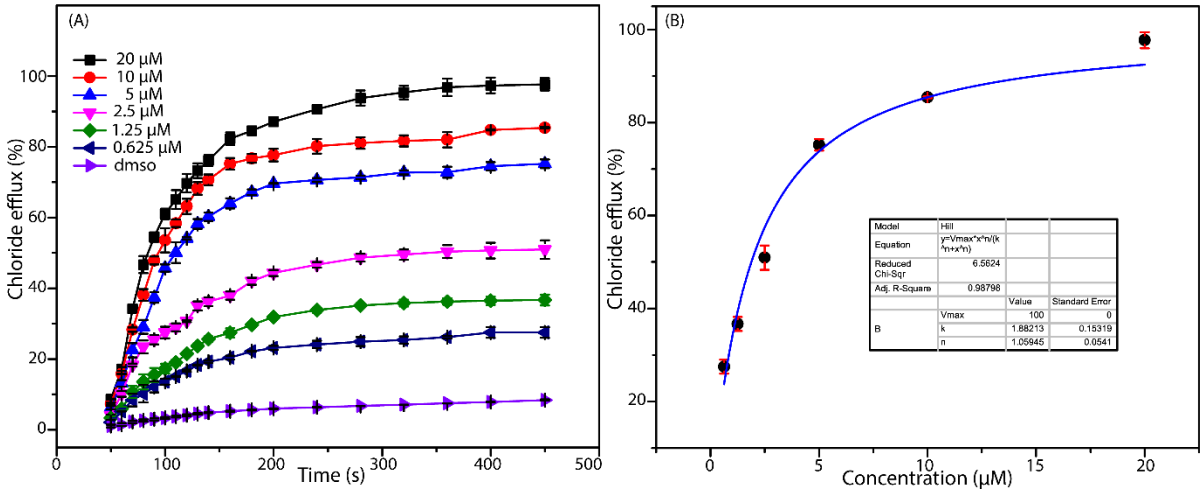

Figure S17. Concentration-dependent transmembrane transport of Cl^- in the presence of **1f** across the DPPC/POPS/CHOL-LUVs⊃lucigenin. The ion transport activity was measured by using Cl-ISE at pH 7.2 (A). The EC_{50} value was calculated using the Hill equation (B). The compound concentration was varied from 20 to 0.625 µM.

6.11. Ion transport activity (HPTS assay) ─ To prepare the solution for the HPTS assay, 1950 µL of 20 mM HEPES buffer, pH 7.2, with 100 mM NaCl, and 40 µL of the DPPC/POPS/CHOL-LUVs⊃HPTS was placed in a 3 mL fluorescence cuvette. The cuvette was then placed in the fluorescence spectrophotometer under slow stirring conditions for 3 to 5 minutes to ensure a homogeneous solution. HPTS fluorescence emission was measured at 506 nm (excited at 455 nm) when the kinetic experiment got underway (at t = 0 s). Following this, the cuvette was maintained in a stirring state with the chamber temperature set to 25 ºC. The compound (10 µL of 10 µM DMSO stock solution) was introduced after 45 s to start the Cl^- inflow kinetics. The vesicles were lysed by adding 20% Triton X-100 (20 L) to the cuvette at t = 450 s to end the kinetic experiment, and fluorescence measurements were conducted for an additional 50 s (t = 500 s).

6.12. Anion selectivity studies ─ The identical procedure outlined above was used to prepare the vesicles. This test used 100 mM of NaX salt solution (where A = F^-, Cl^-, Br^-, I^-, NO_3^- $ClO_4^-$and SCN^-) as an external buffer. At t = 0 s, the suspension was maintained in a gently stirring state in a fluorescence apparatus with a magnetic stirrer. At λ_{em} = 535 nm (λ_{ex} = 455 nm), the quenching of lucigenin's fluorescence intensity was seen with time. the insertion of transporter **1f** at t = 45 s. To fully destroy the imposed Cl^- gradient, vesicles were lysed by the

addition of 20% Triton X-100 (20 µL) at t = 450 s. Using Eq.-S2, the time-dependent data were converted to a percent change in fluorescence intensity.

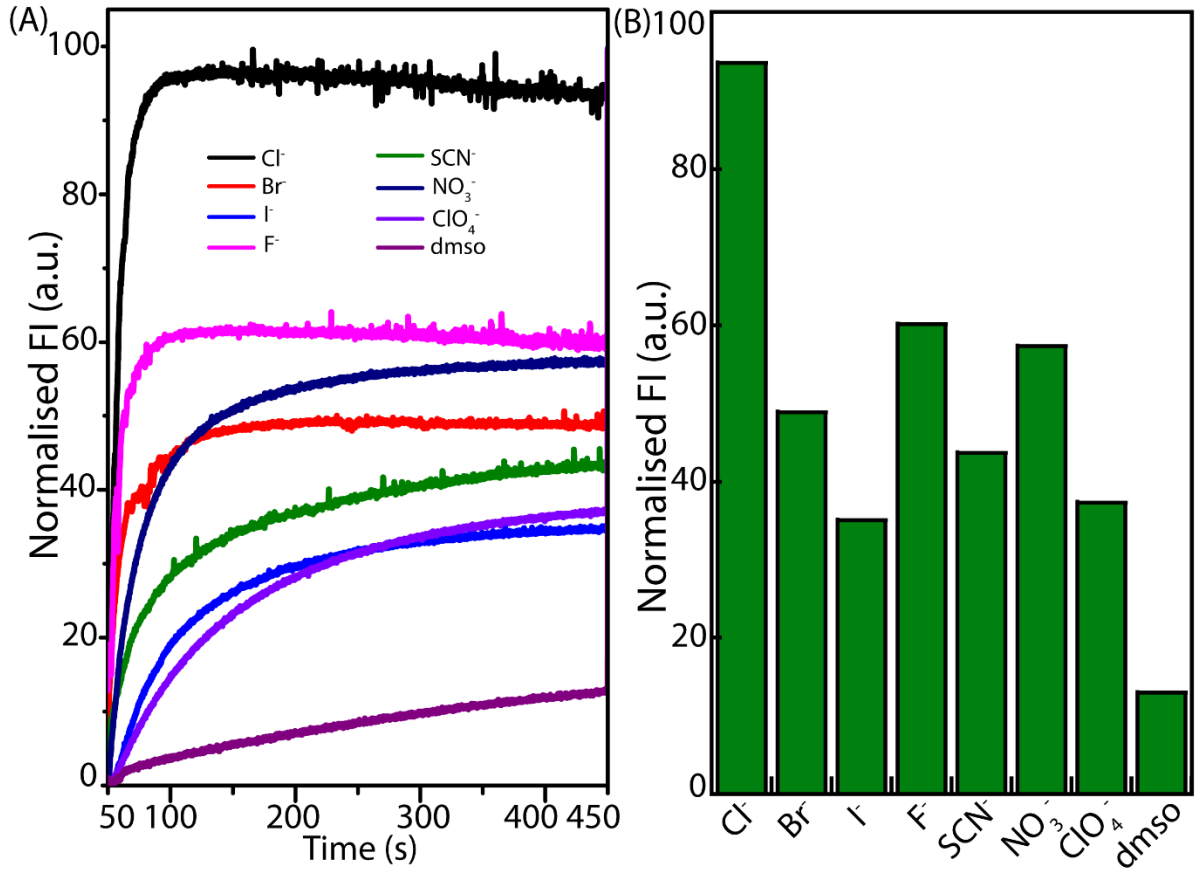

Figure S18. The anion transport selectivity of **1f** (20 µM) across the DPPC/POPS/CHOL-LUVs⊃HPTS (6:2:2 molar ratio) was measured at pH 7.2 (A), percentage of Cl^- efflux in the presence of different anions (B).

6.13. Cation selectivity assay across DPPC/POPS/CHOL-LUVs⊃lucigenin ─ The vesicles were prepared by following the same protocol as stated above. In clean and dry fluorescence cuvette, 20 mM HEPES buffer and 100 mM MCl (M = Li^+, Na^+, K^+, Rb^+, and Cs^+) (1950 µL) and DPPC/POPS/CHOL-LUVs⊃lucigenin (40 µL) were taken.

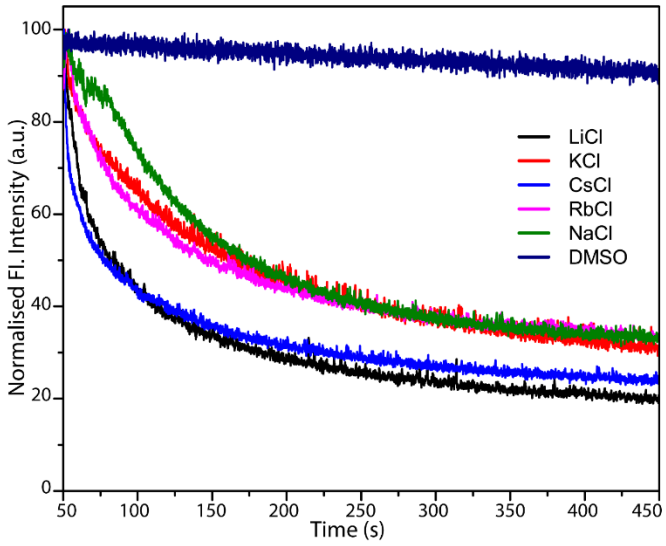

Figure S19. Cation selectivity of **1f** (5 μM) measured by varying external cations (M^+ = Li^+ , Na^+ , K^+ , Rb^+ , Cs^+) across DPPC/POPS/CHOL-LUVs⊃lucigenin.

7. Evidence for the mechanistic pathway for Cl^- transport:

7.1. Ion transport activity in the presence of FCCP (FCCP assay) ─ The ion transport activity was evaluated in the presence and absence of FCCP (H^+ selective transporter). In a 3 mL fluorescent cuvette, 1950 μL of 20 mM HEPES buffer, pH 7.2, including 100 mM NaCl, and 40 μL of the DPPC/POPS/CHOL-LUV⊃HPTS were placed. The cuvette was then placed into the fluorescence equipment and stirred for 3 minutes. The compound **1f** (8 μL of the stock solution in DMSO) and 2 μL of FCCP solution in DMSO (5 μM) were then added to the solution at t = 45 s. After 45 seconds, compound **1f** (final concentration) pulse was introduced to the cuvette to start the Cl^- transfer kinetics. After 450 s, the kinetic experiment was stopped by adding 20 μL of 20% Triton-X100 solution to the cuvette (to rupture the vesicular arrangements), and the fluorescence measurements were continued for another 45 s (t = 500 s). The control experiment was likewise conducted in the absence of FCCP.

7.2. Ion transport activity in the presence of Valinomycin (Valinomycin assay) ─ The vesicles were made using the same method described in the preceding section. The activity of ion transport was evaluated in the absence and presence of valinomycin. In a 3 mL fluorescent cuvette, 1950 μL of 20 mM HEPES buffer, pH 7.2, including 100 mM KCl, and 40 μL of the DPPC/POPS/CHOL-LUV⊃HPTS were placed. The cuvette was then placed into the fluorescence equipment and stirred for 3 minutes. The intensity of the HPTS fluorescence was then measured (t = 0 s) at 510 nm (λ_{ex} = 450 nm). The compound (8 μL of the stock solution

in DMSO) and 2 µL of valinomycin solution in DMSO (10 nM) were then added to the solution at t = 45 s to commence the Cl^- transport kinetics. After 450 seconds, the kinetic experiment was stopped by pouring 20 µL of 20% Triton-X100 solution into the cuvette (to break the vesicular arrangements), and the fluorescence measurements were continued for another 50 s (t = 500 s). The control experiment was likewise carried out in the absence of valinomycin.

7.3. U-tube experiment:

The U-tube experiment was carried out to verify this H^+/Cl^- co-transport (either inflow or efflux) mechanism of the compound in an acidic medium. The left arm of the U-tube was filled with 0.1 M aqueous HCl solution (pH 1.2), while the right arm was filled with isotonic $NaNO_3$ and separated by chloroform (organic layer). The chloroform layer is thought to be a lipid bilayer mimic. The transit of Cl^- and H^+ ions was monitored with a Cl-ISE and a pH meter, respectively. The **1f** (20 µM) was put in the chloroform layer, and measurements were taken for 70 hours.

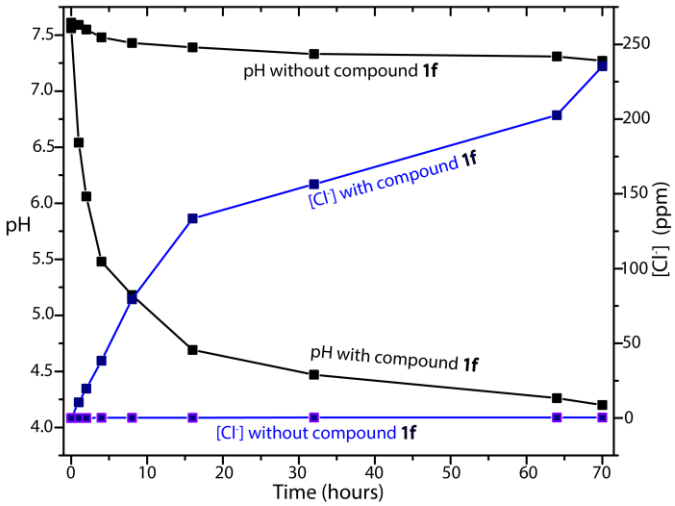

Figure S20. Measurement of the H^+/ Cl^- transport efficacy by **1f** (20 µM) using Cl-ISE and pH-meter across a U-tube.

7.4. Evidence for mobile carrier mechanism:

7.4.1. Transport activity across DPPC-lucigenin assay─ The transport activity of the drugs was evaluated using a fluorescence spectrophotometer in this DPPC-lucigenin experiment. 1950 µL of 20 mM HEPES buffer, pH 7.2, including 100 mM NaCl, and 40 µL of DPPC-LUV⊃lucigenin were placed in a 3 mL fluorescence cuvette for this test. The kinetic experiment began (at t = 0 s), and the emission of lucigenin fluorescence was measured at 506

nm (excited at 455 nm). The cuvette was then stirred, and the chamber temperature was adjusted to 25 ºC. After 45 s, the compound (10 µL of DMSO stock solution) was introduced to begin the Cl^- inflow kinetics. Finally, at t = 450 s, the vesicles were lysed by adding 20% Triton X-100 (20 µL) to the cuvette, and fluorescence measurements were continued for another 50 s (t = 500 s). A comparable measurement was carried out to assess the transport efficiency at 45 ºC. To calculate the half-life and starting rate at different temperatures, the time-dependent lucigenin fluorescence plot was fitted with a first-order exponential decay equation.

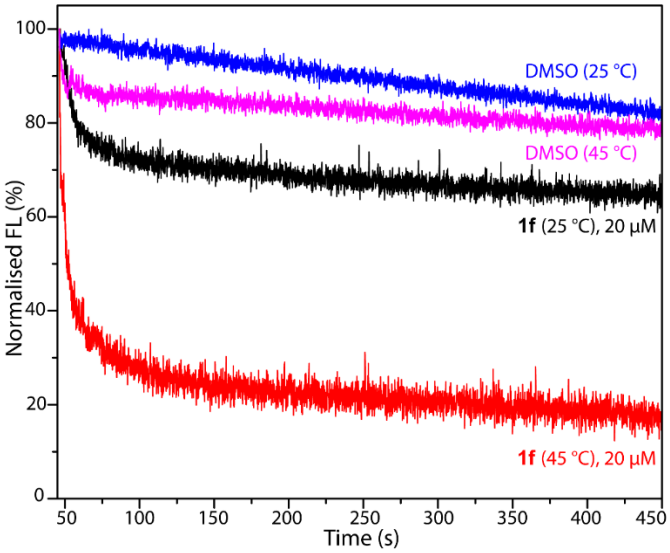

Figure S21. Temperature-dependent Cl^- transport by **1f** (20 µM) using DPPC-LUV⊃lucigenin.

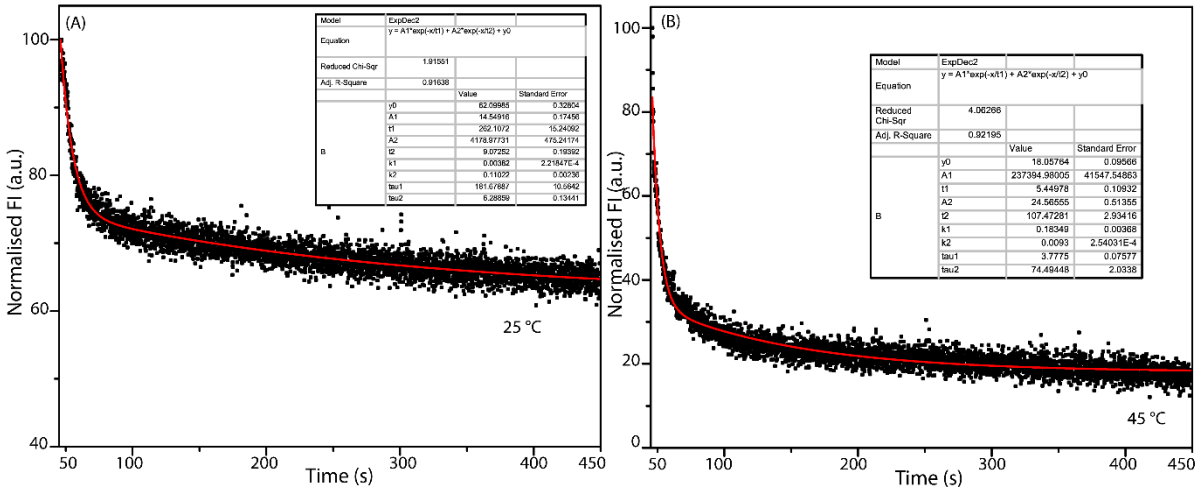

Figure S22. Normalized fluorescence quenching curves (F/F_0) were fitted to an exponential decay 2 equation.

7.5. Preparation of DPPC/POPS/CHOL-LUV⊃CF:

A thin lipid film was prepared by evaporating a solution of DPPC/POPS/CHOL in 0.5 ml $CHCl_3$ in vacuo for 4 h. After that lipid film was hydrated with 0.5 mL buffer (20 mM HEPES, 100 mM NaCl, 50 mM Carboxyfluorescein (CF), pH 7.2) for 1 hour with occasional vortexing of 3-5 times and then subjected to freeze-thaw cycle (≥ 15 times). The vesicle solution was extruded through a polycarbonate membrane with 200 nm pores 19-21 times (it must be an odd number) to give vesicles with a mean diameter of ~ 200 nm. Size exclusion chromatography (Sephadex G-50) with 20 mM HEPES buffer (100 mM NaCl, pH 7.2 final) was used to remove the extracellular dye. Final concentration: ~25 mM lipid; intravesicular solution: 20 mM HEPES, 100 mM NaCl, 50 mM CF, pH 7.2; extravesicular solution: 20 mM HEPES, 100 mM NaCl, pH 7.2.

7.6. Carboxyfluorescein (CF) leakage assay — In a clean and dry fluorescence cuvette, 40 µL of the aforementioned lipid solution and 1950 µL of 20 mM HEPES buffer (100 mM NaCl, pH 7.2) were mixed slowly by a magnetic stirrer fitted with the fluorescence equipment (at t = 0 s). The temporal path of CF fluorescence emission intensity, F_t, was recorded at λ_{em} = 517 nm (λ_{ex} = 492). The compound was added at t = 50 s, and finally, at t = 450 s, 20 µL of 20% Triton X-100 was injected to lyse those vesicles for 100% Cl^- inflow. Fluorescence intensities (F_t) were normalized to fractional emission intensity (IF) using Eq. S2. This investigation demonstrated that neither the bilayer membranes damaged nor large transmembrane pores were generated by **1f.**

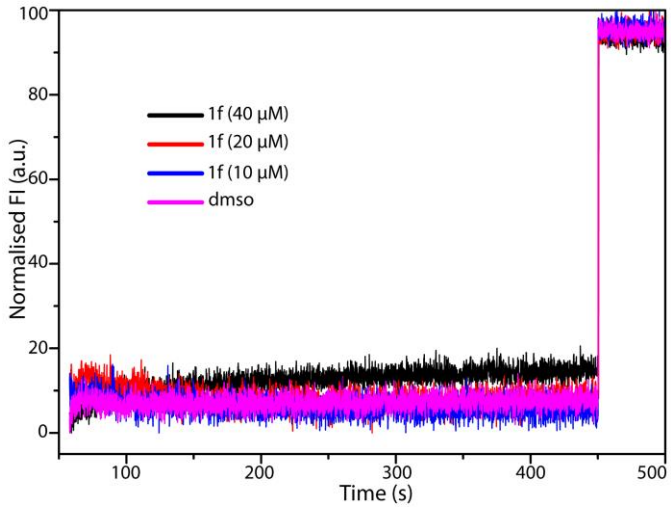

Figure S23. The carboxyfluorescein leakage assay of **1f** across DPPC/POPS/CHOL-LUV⊃CF.

8. pKa determination of by UV-Visible titration:

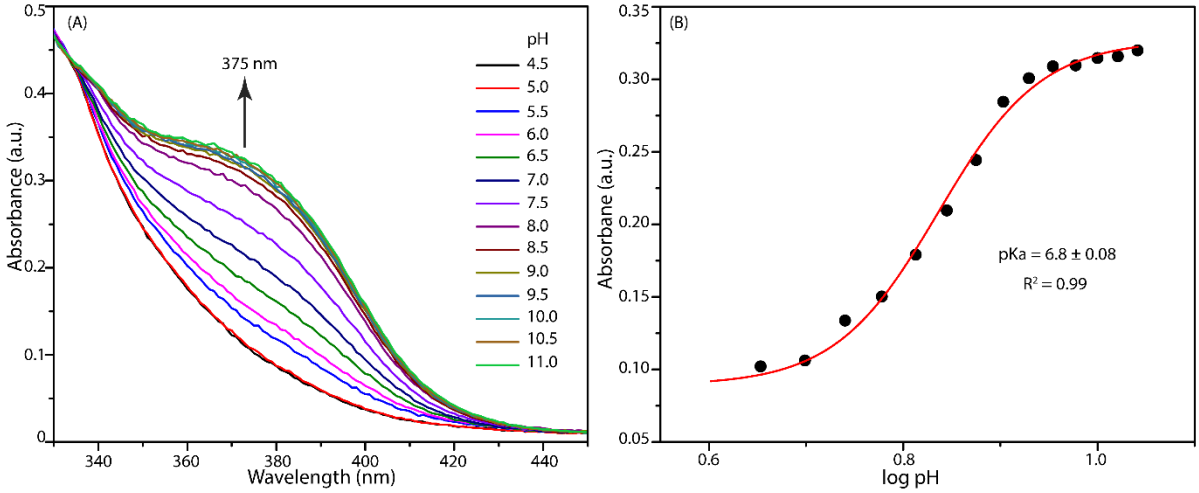

Figure S24. Absorbance spectra of **1f** (20 µM) at different pH in 9:1 DMSO/H_2O (v/v) solution containing 0.1 M NaCl (A). Comparison plots of absorbance at 375 nm at different pH (B).

9. Antibacterial activity studies:

Using the micro broth dilution method, the antibacterial efficacy of the compound was assessed against gram-positive (*S. aureus* (MTCC 96) and MRSA) and gram-negative strains (*E. coli* (MTCC 1687)). The MIC values were calculated as the lowest concentration at which visible growth of the microorganism is inhibited. The assay was performed according to the CLSI guidelines. At 37 °C and 180 rpm, the bacteria were grown in an LB medium (Luria Bertani Broth). As soon as the desired optical density had been attained, the bacteria were centrifuged and washed with distilled water before being diluted to 10^6 CFU/mL in an LB medium. Serial dilution of the compound was performed in a 96-well plate using a micropipette. The cells were added to the serially diluted solution of the compound and incubated at 37 °C for 14-16 hours. Following incubation, the OD_{600} was measured with a BioTek Epoch microplate reader to determine the MIC. In order to obtain the most accurate MIC values, this assay was repeated at different concentration ranges. The error value was calculated as the standard deviation obtained through the mean of the repeated assay results.

To assess the bactericidal activity, 10 µL of the culture from MIC wells exhibiting visibly inhibited growth were subsequently transferred into 100 µL of a fresh medium within neighbouring wells. The 96 well-plate was then incubated at 37 °C for a duration of 24 hrs, following which the optical density was determined at a wavelength of 600 nm.

Simultaneously, 10 µL of culture was taken from the well with the MIC concentration and plated on an agar plate for the duration of 24 hours to determine the bactericidal activity.

Table S2. Antibacterial activity of the compounds.

MIC (µM)			
Compounds	*S. aureus* (MTCC 96)	MRSA (ATCC 33592)	*E. coli* (MTCC1687)
1a	>50	-	-
1b	>50	-	-
1c	>50	-	-
1d	>50	-	-
1e	20.0 ± 5.00	10.0 ± 2.50	>100
1f	2.34 ± 0.39	2.50 ± 0.50	>100
2a	>50	-	-
2b	>50	-	-
4	12.75 ± 1.25	-	-
5	15.625 ± 3.125	-	-
2-(2-aminophenyl)quinazolin-4-amine	>75	-	-
2-(quinazolin-2-yl)aniline	>75	-	-

Figure S25. Minimum bactericidal concentration of **1f** at MIC concentration.

9.1. Time-kill assay:

This study aimed to evaluate the antibacterial activity of the tested compound over the specified duration. The *S. aureus* (MTCC 96) cells were cultured until they had reached the mid-logarithmic phase of their growth. The inoculum was prepared by diluting the culture in LB

medium to obtain an optical density of 0.1. The compound was prepared in PBS buffer together with LB medium in a final concentration of 10 × MIC (20 μM). After the addition of the inoculum, samples were incubated at 37 °C and 180 rpm. Samples were collected at different time points (0, 1, 2, 4, 8, and 12 hours) and stored at -20 °C. Once all samples were collected, they were centrifuged at 5000 rpm for 5 minutes, and the supernatant was removed. The samples were then diluted three-fold and inoculated onto agar plates using a spreader. The plates were then incubated overnight at 37 °C, and the resulting colonies were counted manually to determine the colony-forming units per millilitre (CFU/mL).

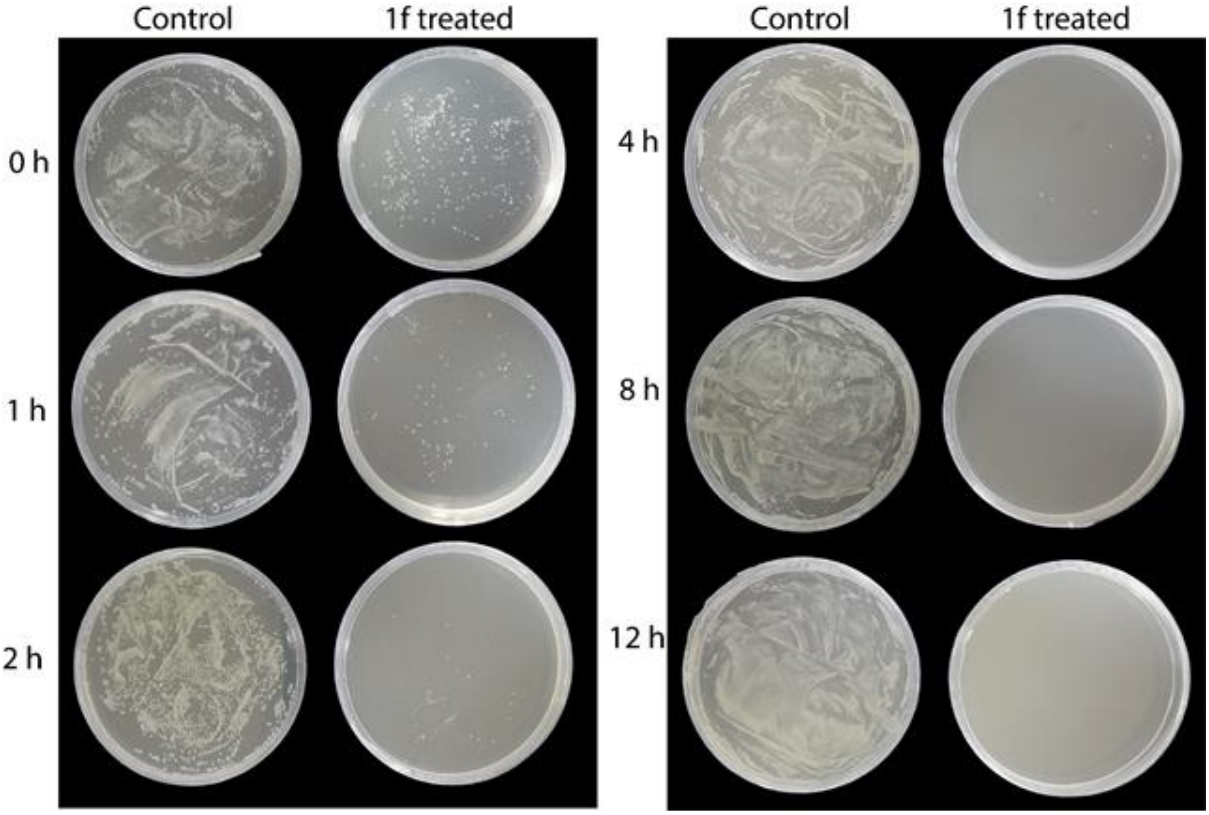

Figure S26. Bacterial growth on agar plates after a differential period of time.

Note: The viability of *S. aureus* cells was measured at different time intervals in order to determine the bactericidal effect of the compound. Figure S25 revealed that the compound exhibited bactericidal activity after 8 hours of incubation. The CFU/mL (colony forming units per millilitre) were calculated while taking the dilution factor into consideration. The dilution factor is the proportion of the original sample volume to the volume plated on the agar plate.

$$CFU/mL = \frac{No.of\ colonies \times dilution\ factor}{Volume\ of\ culture\ plated\ (in\ mL)} \qquad Eq.\ S3$$

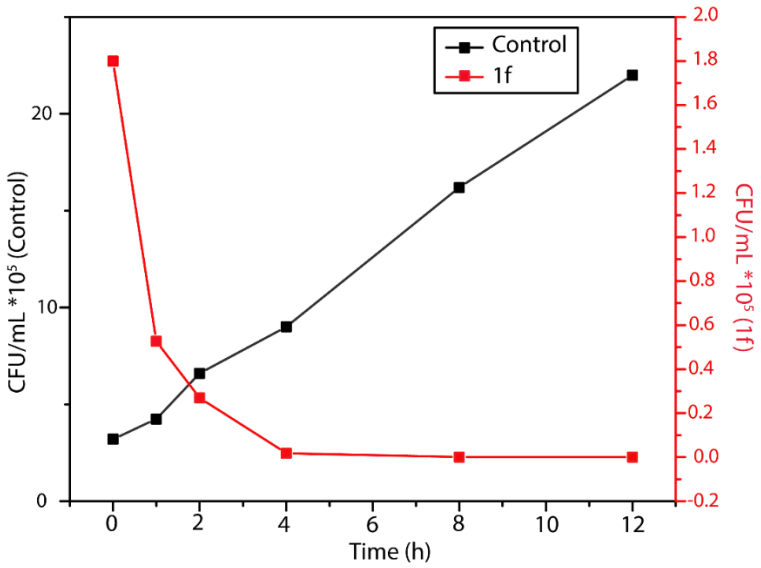

Figure S27. Time-kill curve showing changes in CFU of control and compound treated bacteria culture over time.

9.2. Morphological study:

Morphological analysis of bacterial cells treated with the compound was performed using a field emission scanning electron microscope (FESEM). To prepare the samples for FESEM imaging, *S. aureus* cells were cultured until they reached the mid-logarithmic growth phase and then harvested by centrifugation at 5000 rpm for 5 minutes. The cells were then washed and treated with **1f** (at MIC concentration). A bacterial culture without treatment with the compound was retained as a control. After 3 hours of incubation, the cell pellets were collected by centrifugation, washed with PBS buffer, and dropped onto a glass grid covered with aluminium foil. A laminar airflow was used to air dry the sample. The drop cast sample was then mounted on a metal FESEM grid held in place with carbon tape. The sample was gold-plated twice before FESEM analysis. This preparation process facilitated the study of the morphology of the bacterial cells using FESEM. It allowed for a detailed characterization of any structural changes induced by the compound treatment.

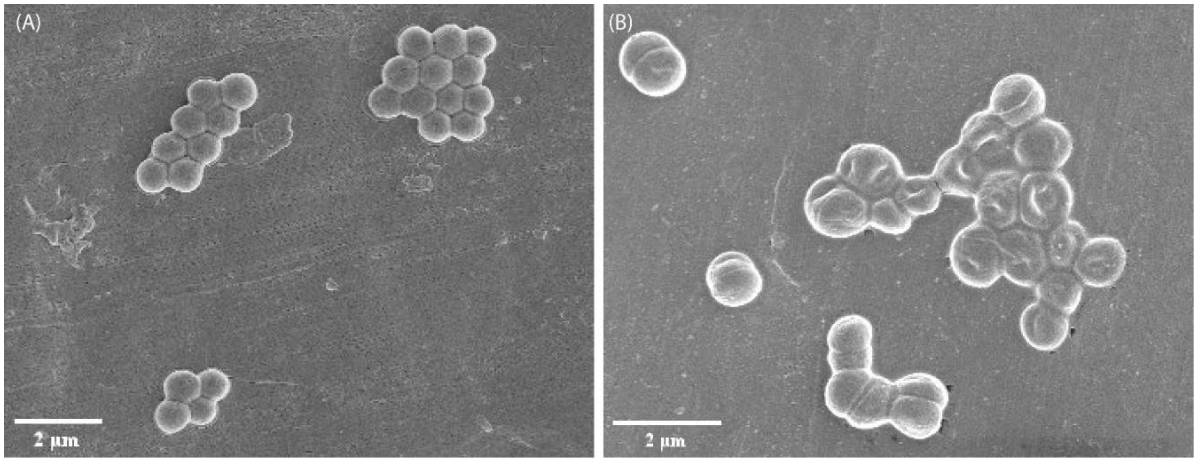

Figure S28. Morphological analysis of *S. aureus* cells. Control (A) and **1f** (B) treated *S. aureus* cells.

9.3. MQAE Assay:

This assay has been performed to analyze Cl^- transport in bacterial cells. The MQAE dye (N-(ethoxycarbonylmethyl)-6-methoxyquinolinium bromide) is a specific Cl^--sensing dye used to analyze Cl^- transport in cells due to its cell permeability.[3] *S. aureus* cells were grown in LB medium in the presence of MQAE (1 mM) in an incubator shaker at 37 °C and 180 rpm for 14-16 hours. The cells were then washed, collected, and resuspended in 10 mM HEPES and 50 mM NaCl buffer (pH: 7.2) to estimate intracellular Cl^- transport. For this assay, 150 µL of resuspended bacterial culture was mixed in 1850 µL of buffer (10 mM HEPES and 50 mM NaCl, pH 7.2) in a clean and dry fluorescence cuvette and kept under slow stirring conditions, and the fluorescence intensity of MQAE within the cells was monitored at 450 nm (λ_{ex}: 350 nm). At t = 100s, **1f** was added at a concentration of 20 µM, and the MQAE fluorescence intensity was monitored for a further 900s. The same was performed for the control; 0.5% DMSO was added.

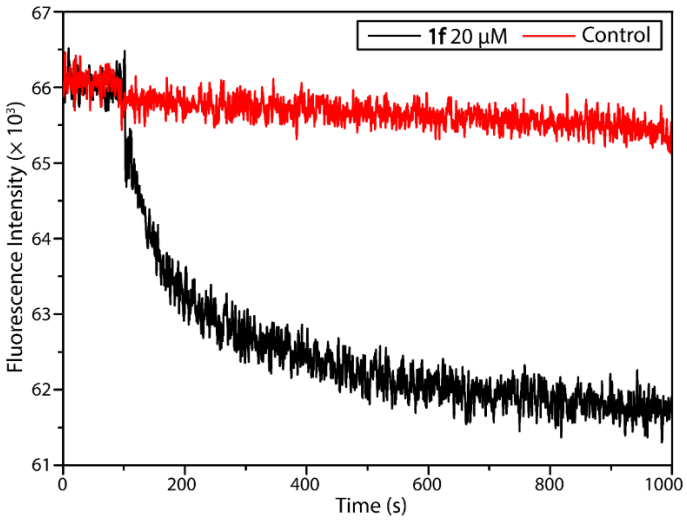

Figure S29. MQAE-based fluorescence assay. At t = 100s, the compound was the bacterial cells, and a decrease in fluorescence intensity was observed.

Note: This study aimed at assessing transmembrane Cl^- transport properties of the bacterial cells in the presence of **1f** using the MQAE (cell permeable) dye.[3] Bacterial cells were exposed to the dye, which was internalized by the cells. As Cl^- was transported into the cytoplasm of the bacterial cells, the fluorescence intensity of the dye was quenched. The addition of **1f** enhanced the rate of Cl^- transport within the cells, resulting in a time-dependent drop in fluorescence intensity. This result suggests that **1f** could rapidly transport Cl^- across bacterial cell membranes, as evidenced by a decrease in fluorescence intensity.

10. NMR spectra of synthesized compounds:

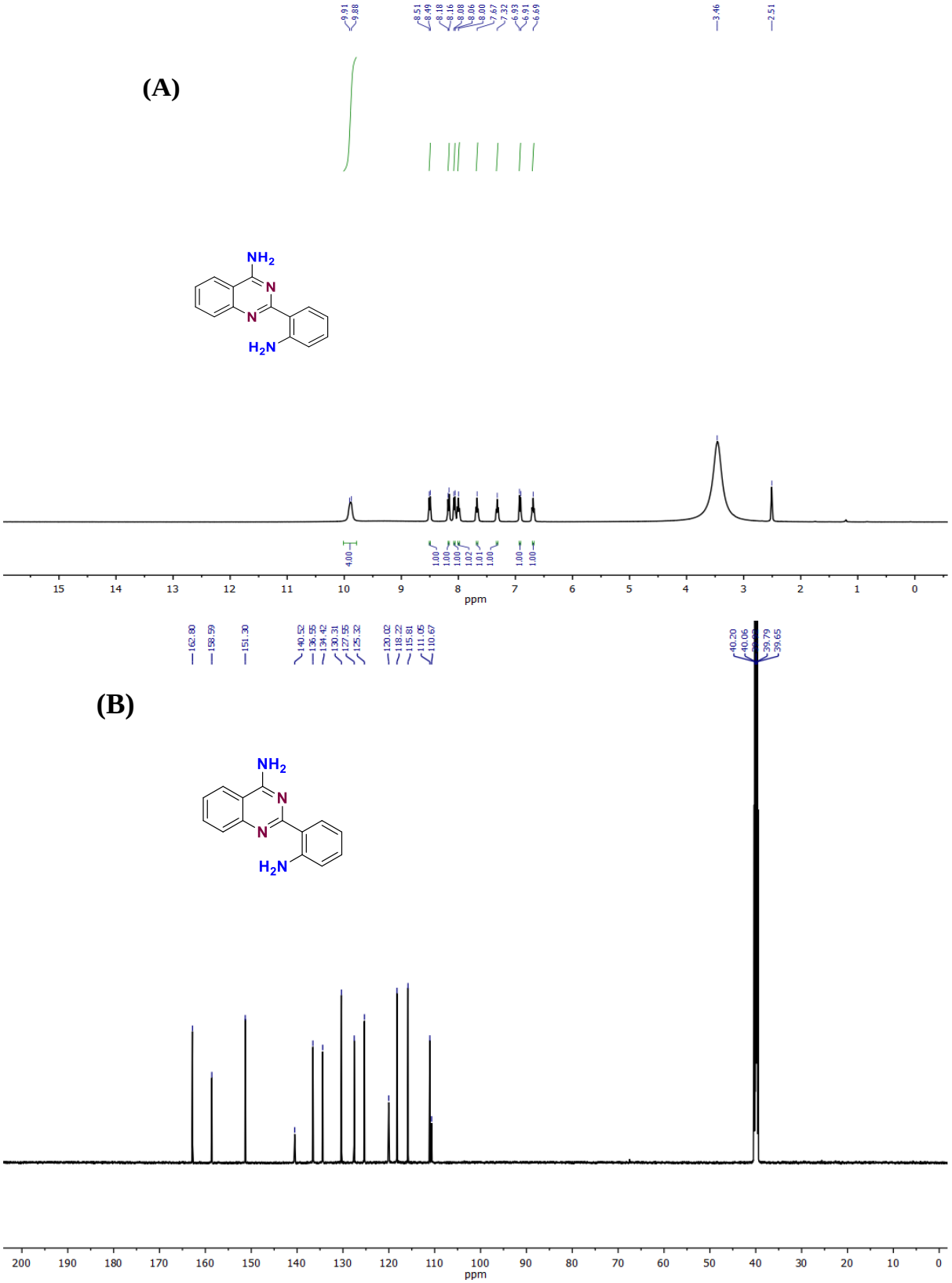

Figure 30. ^{1}H NMR (A) and ^{13}C NMR (B) spectra of 2-(2-aminophenyl)quinazolin-4-amine in the DMSO-d_6 solvent.

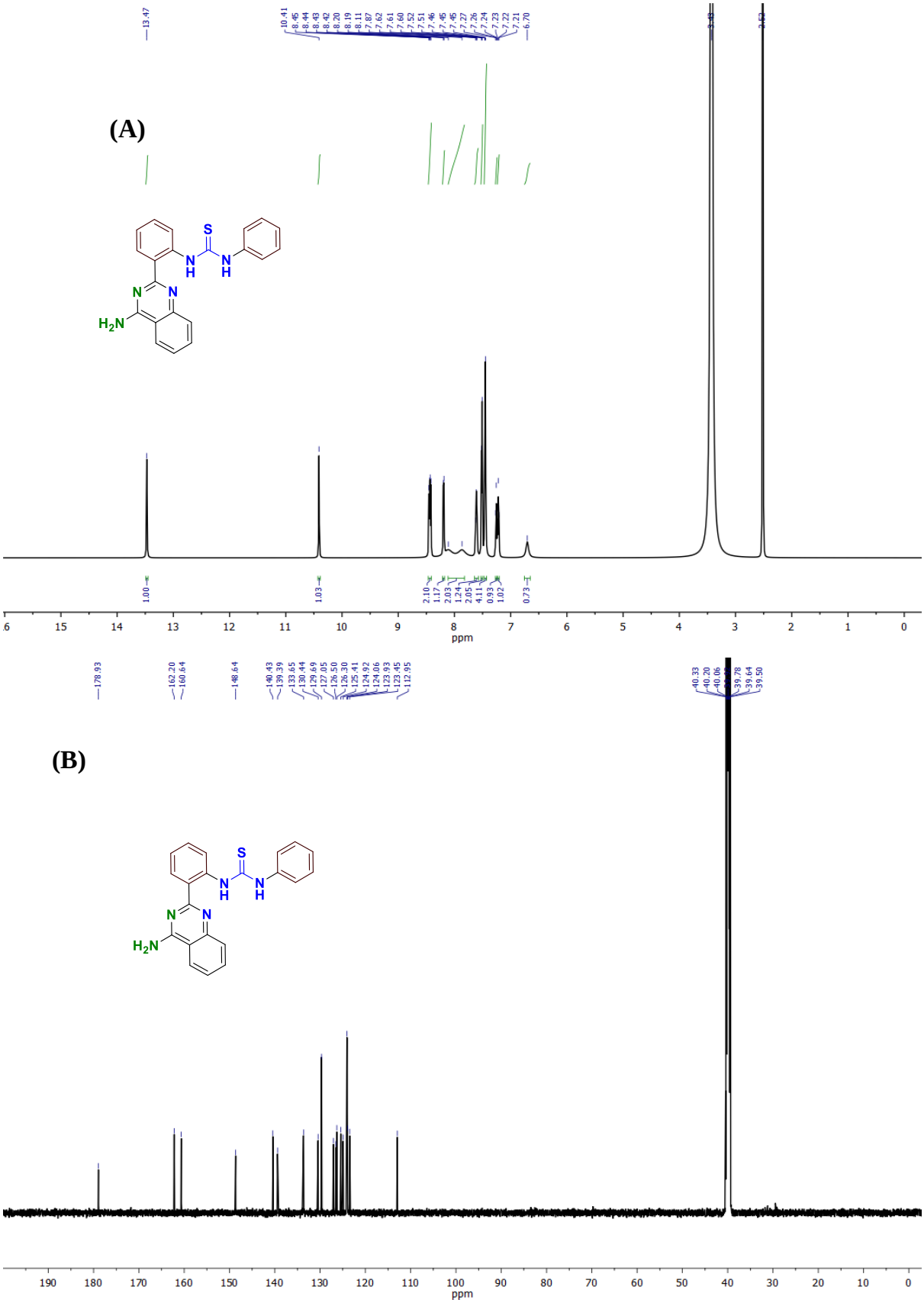

Figure S31. ^{1}H NMR (A) and ^{13}C NMR (B) spectra of **1a** in the DMSO-d_6 solvent.

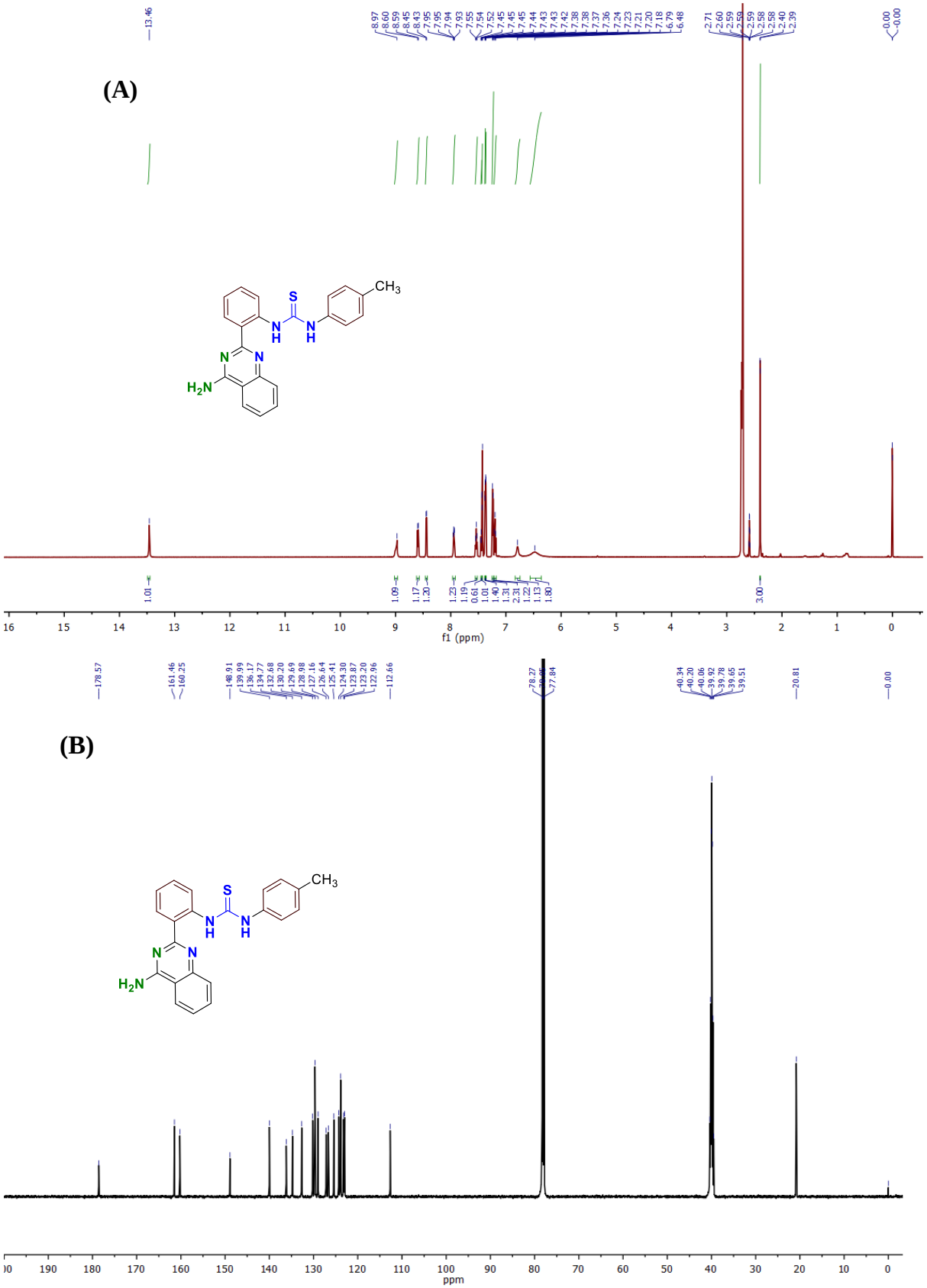

Figure S32. ^{1}H NMR (A) and ^{13}C NMR (B) spectra of **1b** in the $CDCl_3$ + DMSO-d_6 solvent.

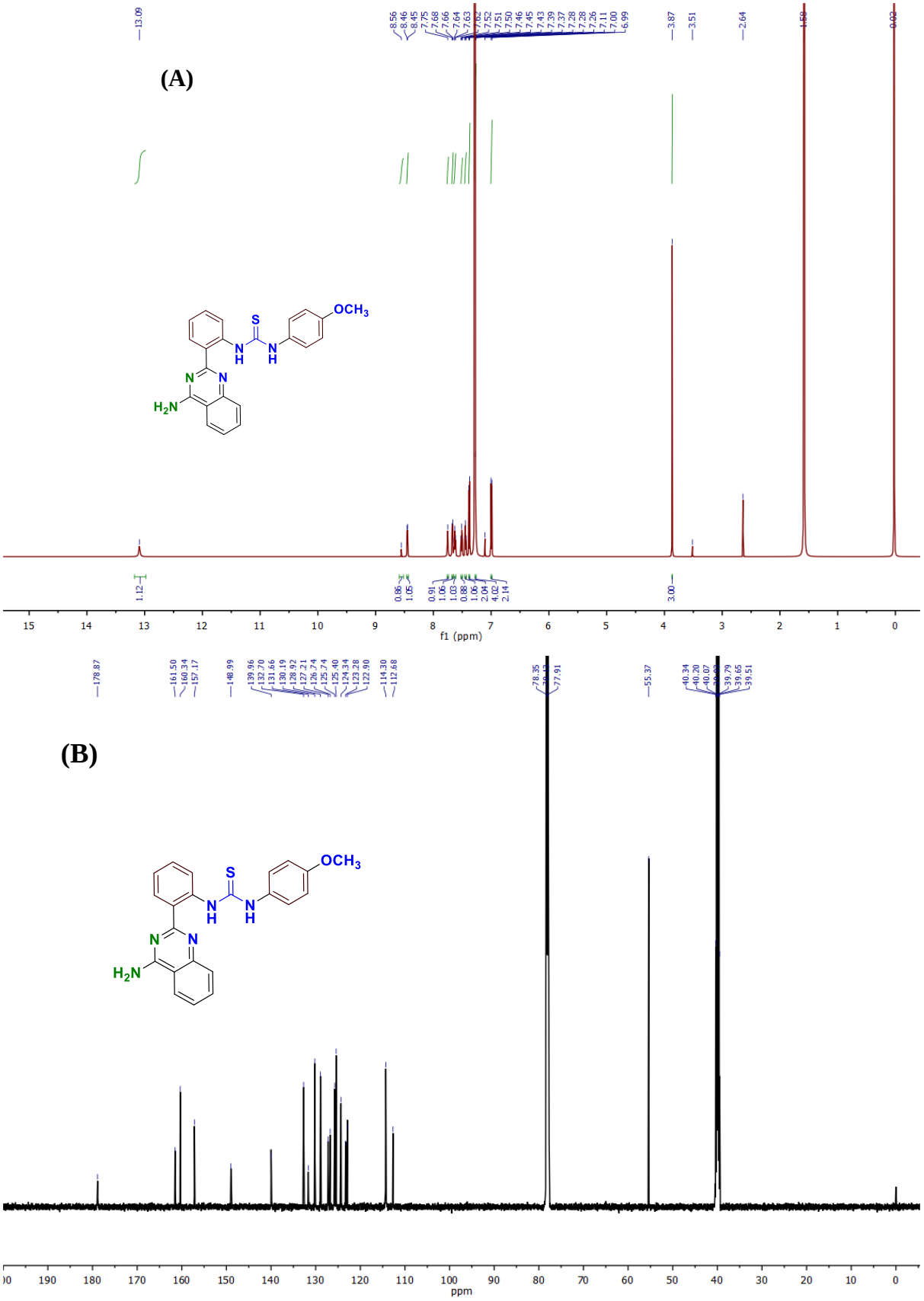

Figure S33. ^{1}H NMR (A) and ^{13}C NMR (B) spectra of **1c** in the $CDCl_3$ + DMSO-d_6 solvent.

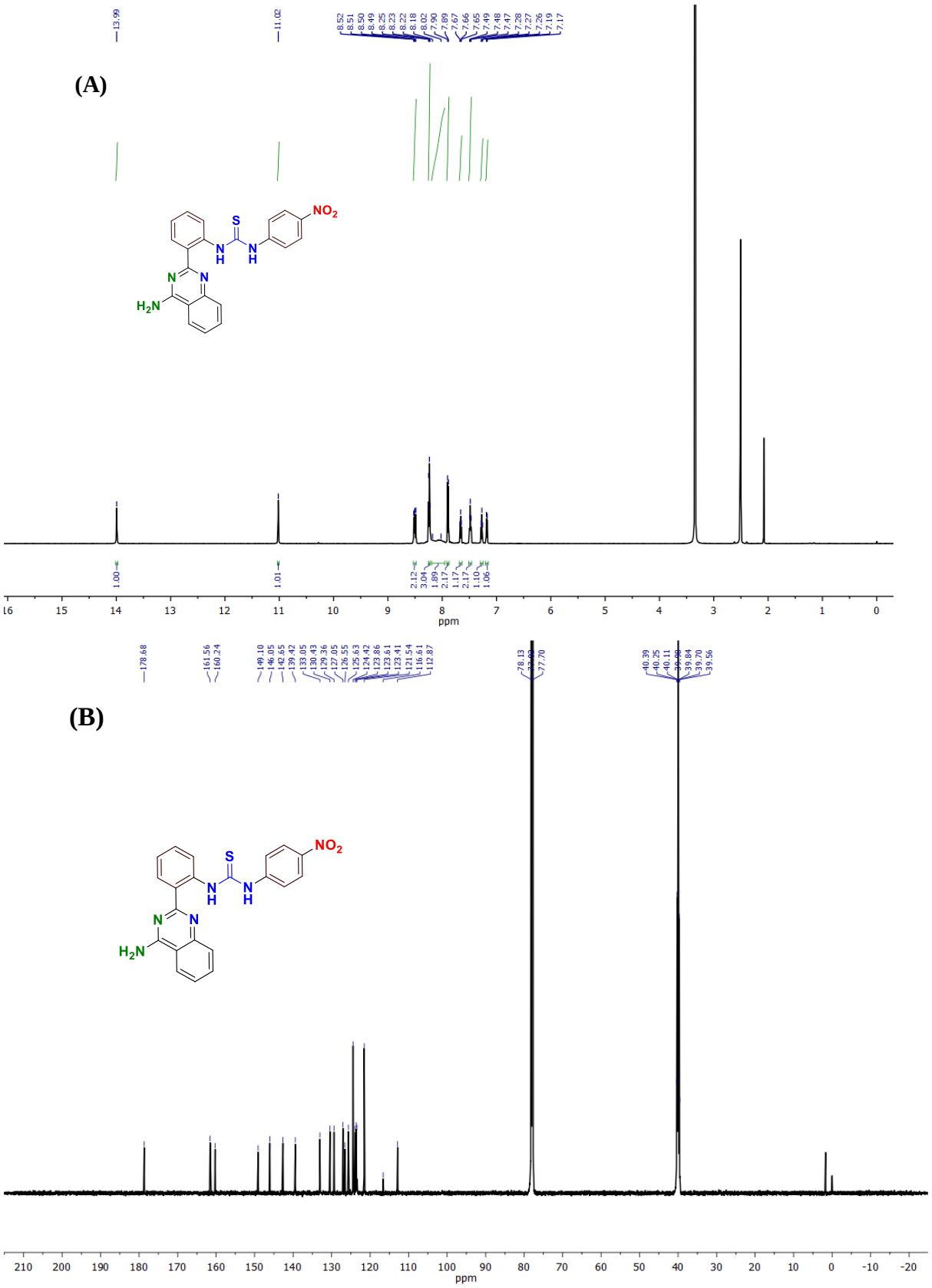

Figure S34. ^{1}H NMR (A) and ^{13}C NMR (B) spectra of **1d** in the $CDCl_3$ + DMSO-d_6 solvent.

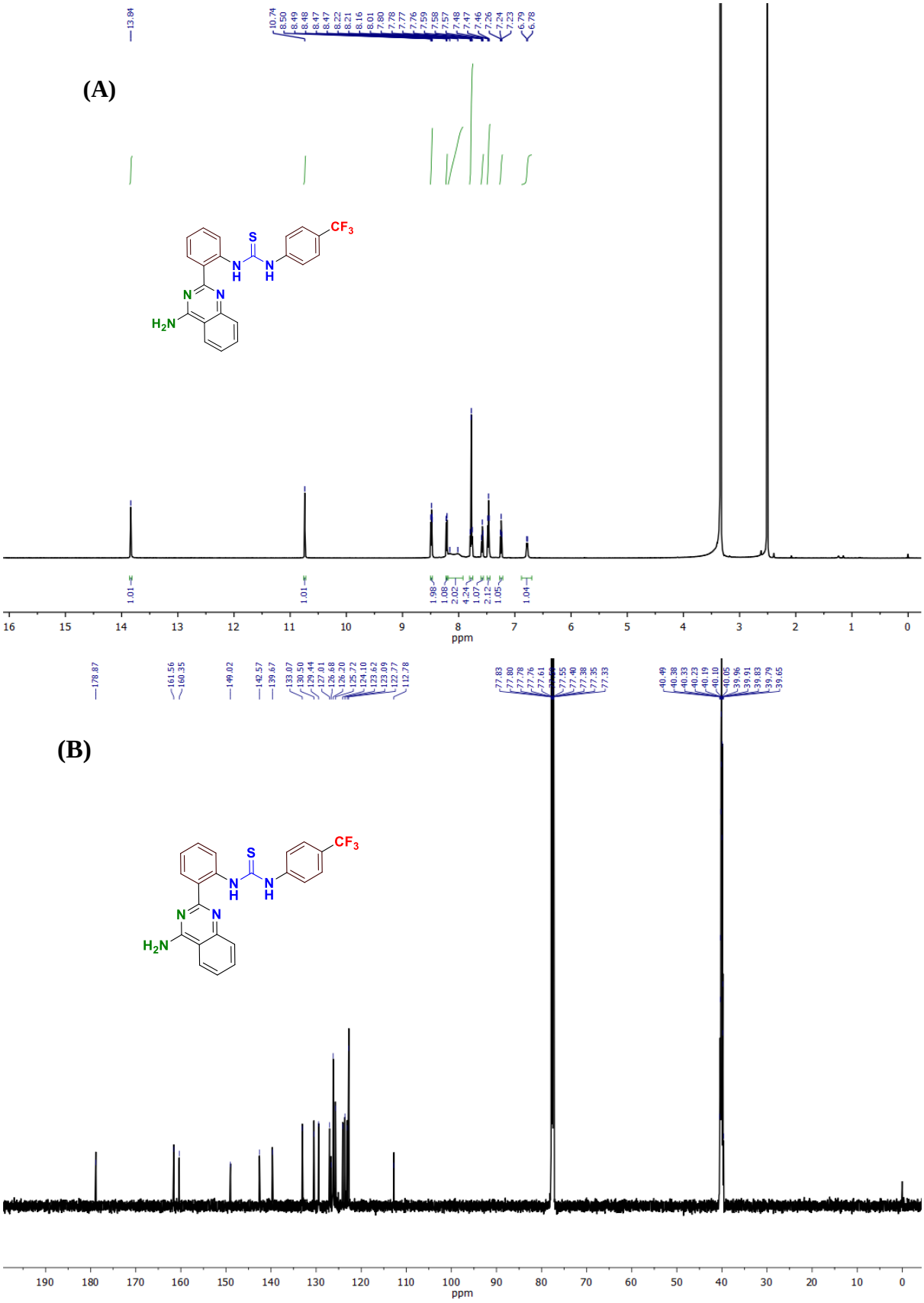

Figure S35. ^{1}H NMR (A) and ^{13}C NMR (B) spectra of **1e** in the DMSO-d_6 solvent.

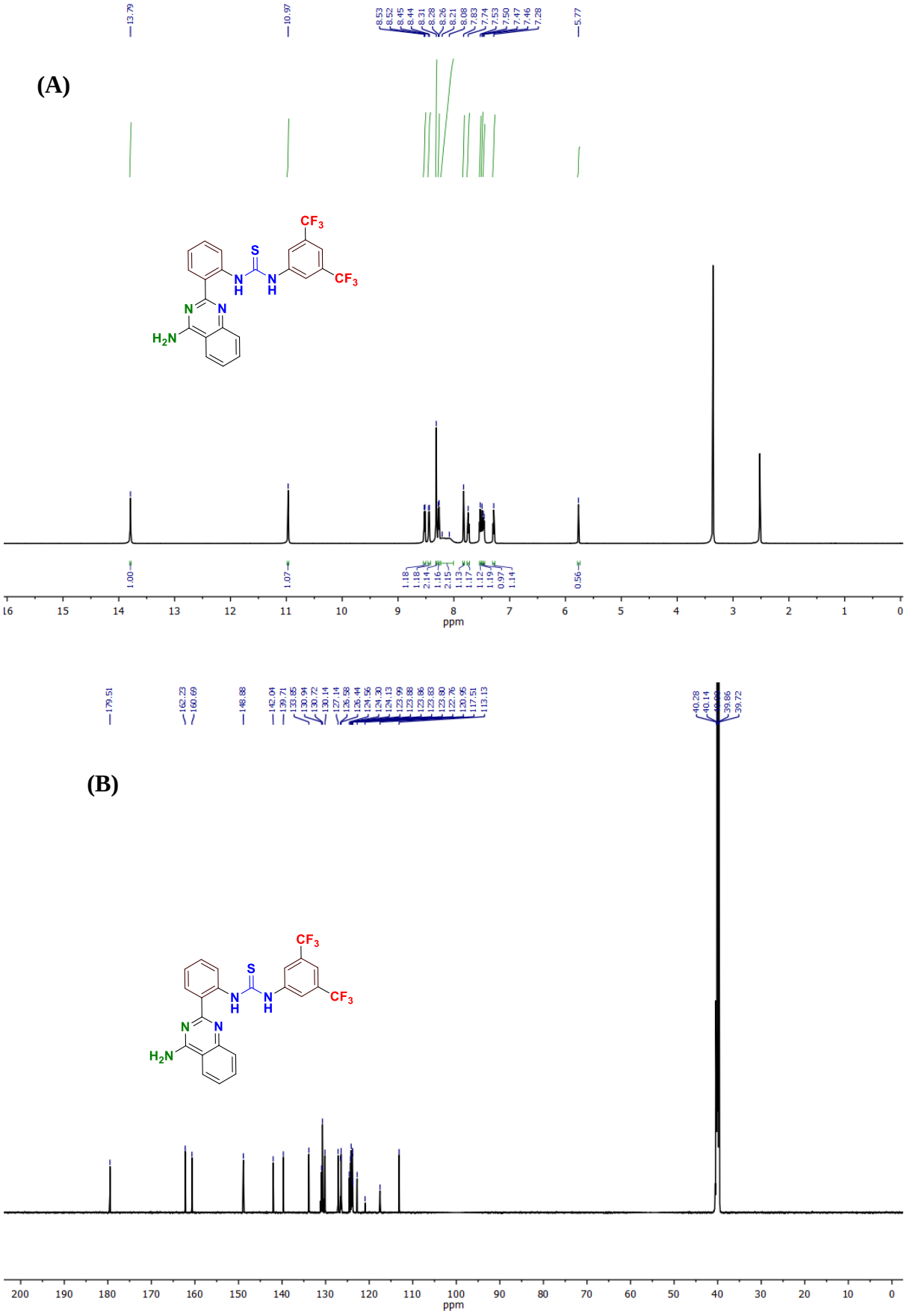

Figure S36. ^{1}H NMR (A) and ^{13}C NMR (B) spectra of **1f** in the DMSO-d_6 solvent.

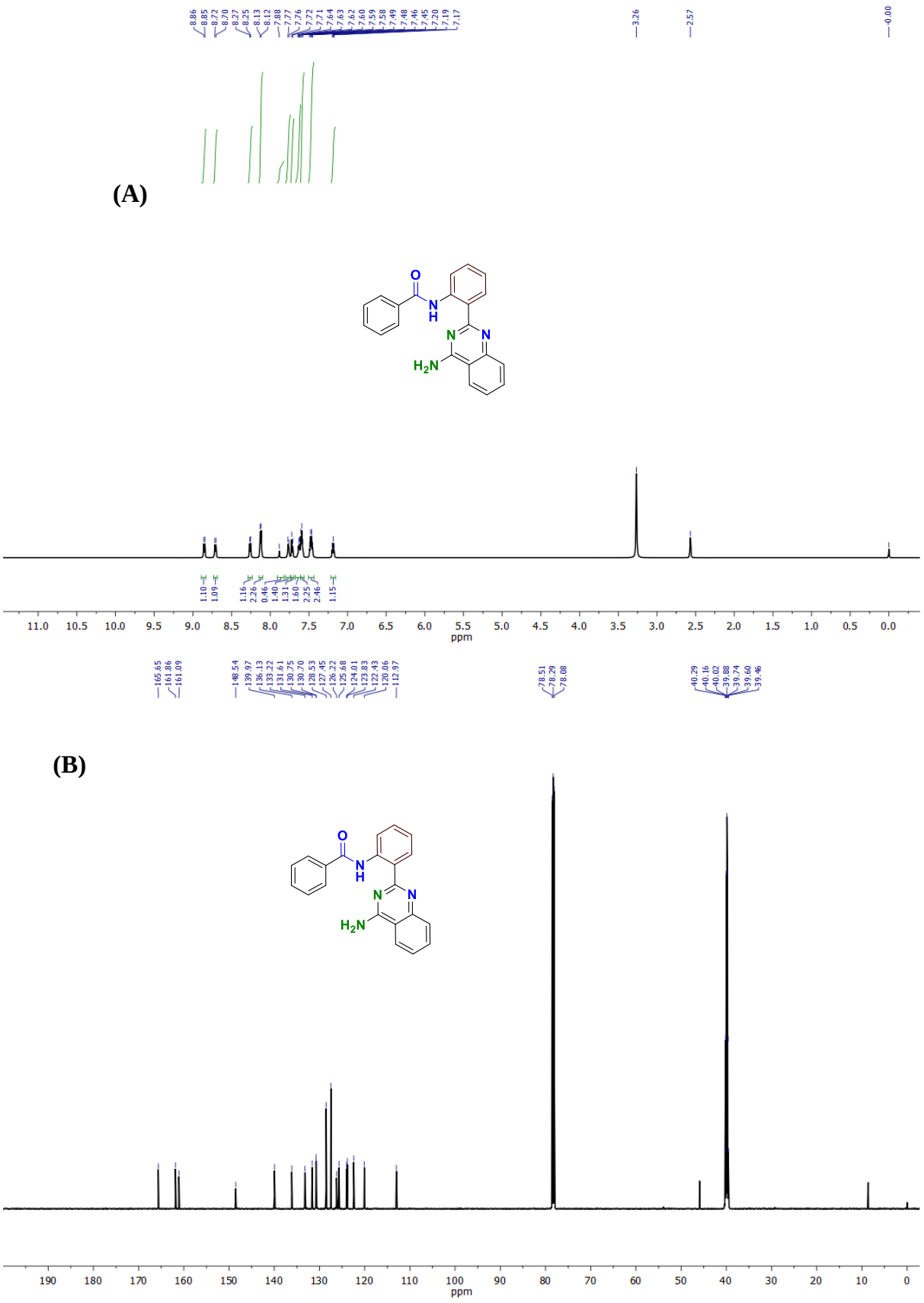

Figure S37. ^{1}H NMR (A) and ^{13}C NMR (B) spectra of **2a** in the $CDCl_3$ + DMSO-d_6 solvent.

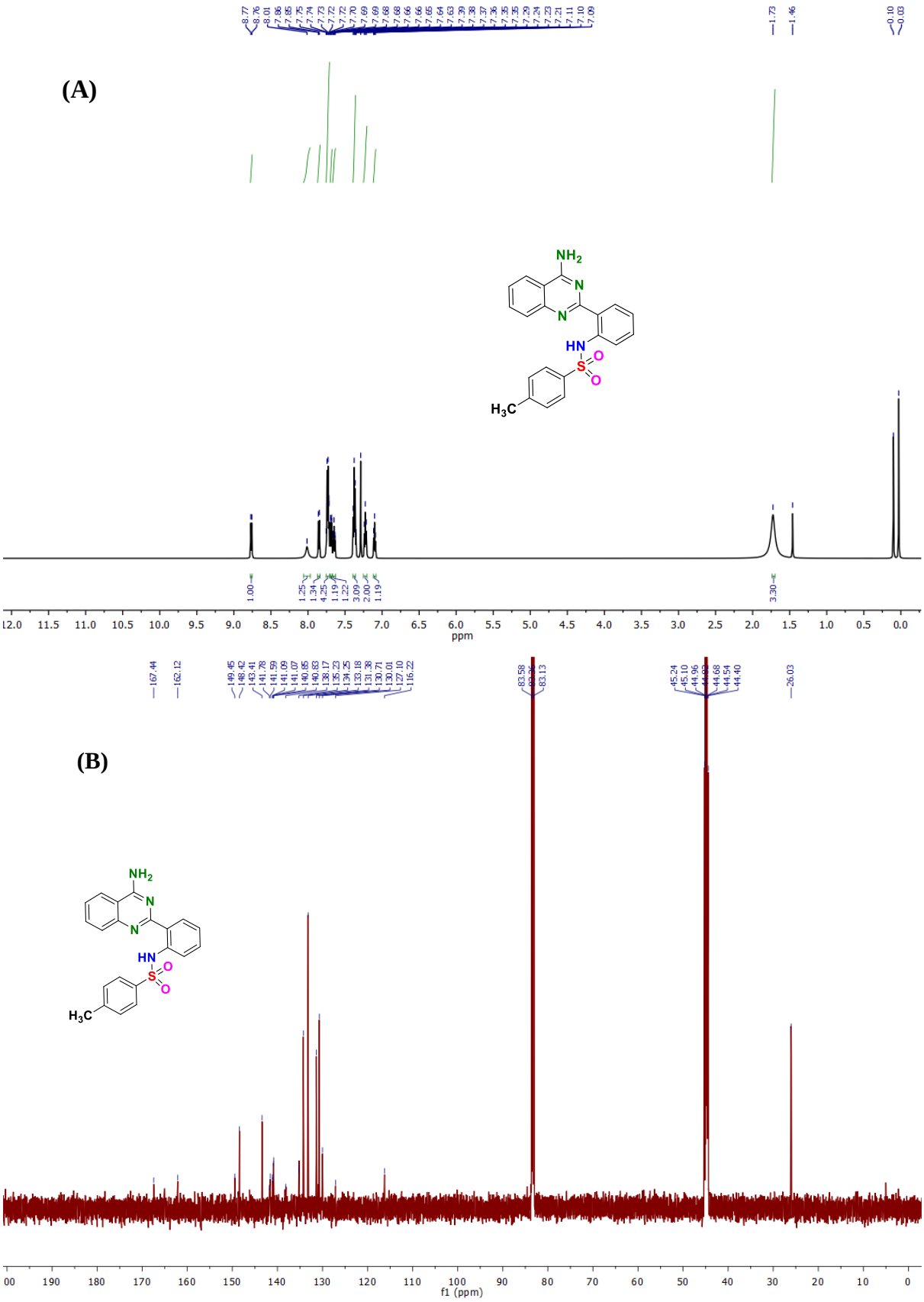

Figure S38. ^{1}H NMR (A) and ^{13}C NMR (B) spectra of **2b** in the $CDCl_3$ + DMSO-d_6 solvent.

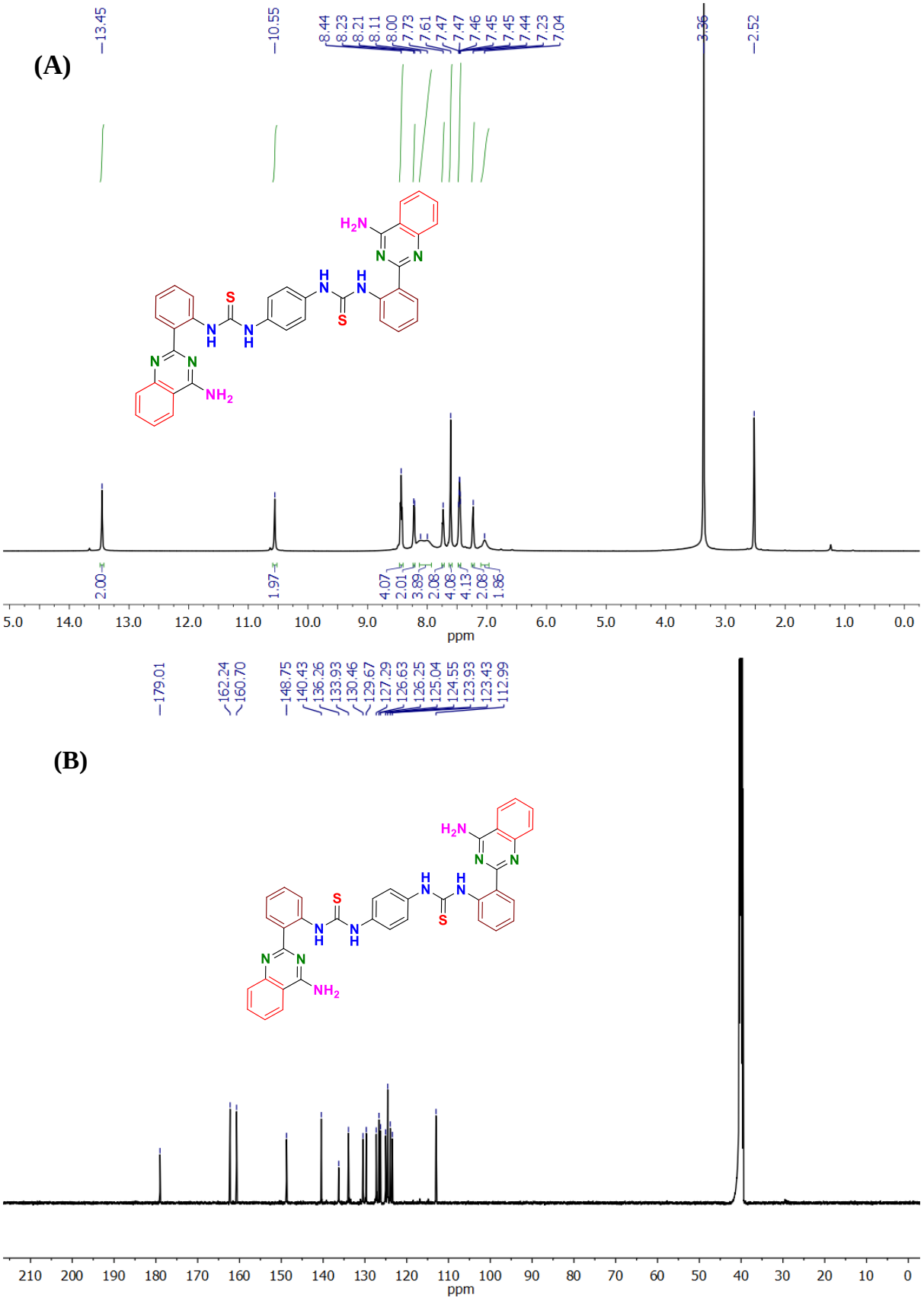

Figure S39. ^{1}H NMR (A) and ^{13}C NMR (B) spectra of **3a** in the DMSO-d_6 solvent.

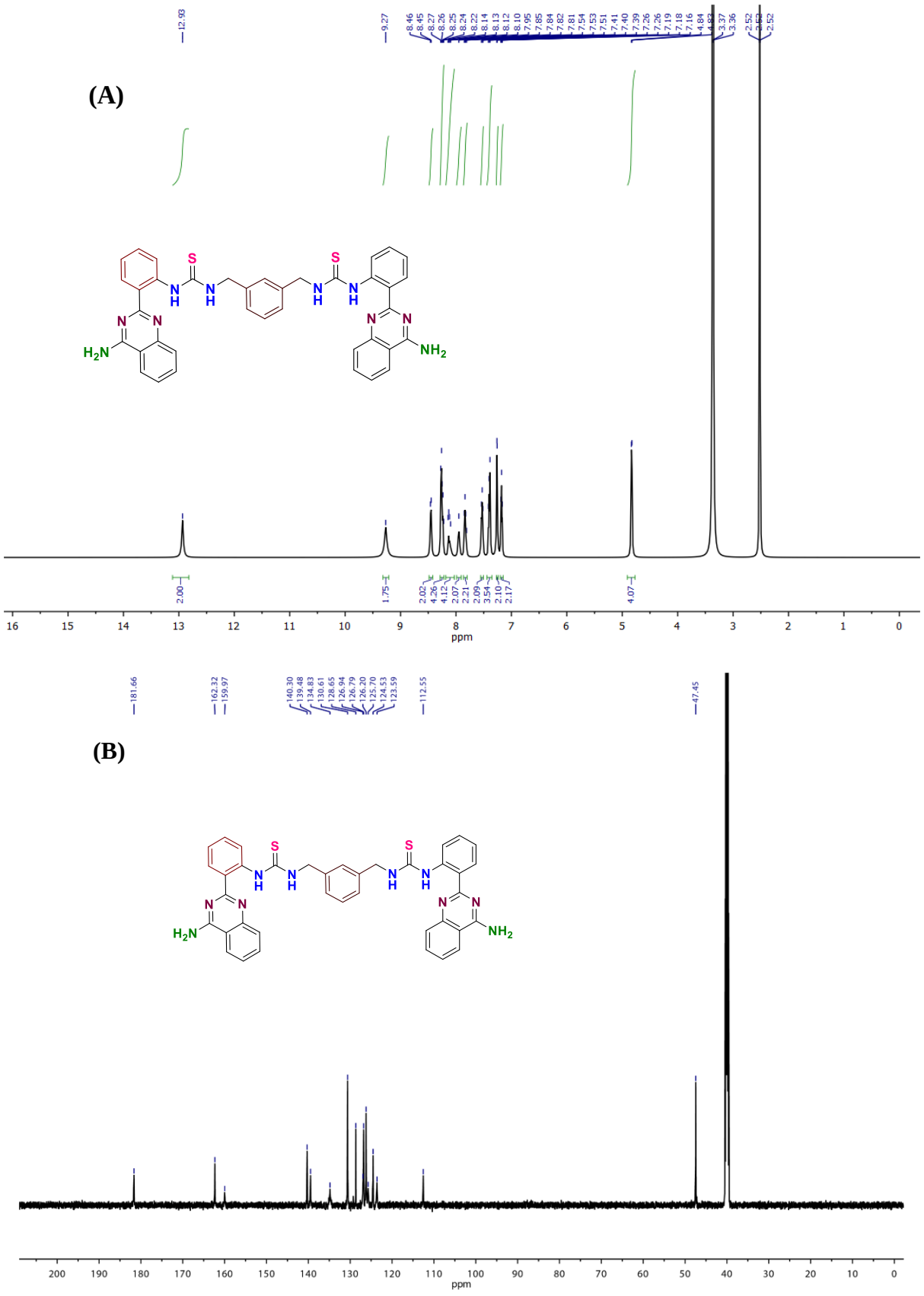

Figure S40. ^{1}H NMR (A) and ^{13}C NMR (B) spectra of **3b** in the DMSO-d_6 solvent.

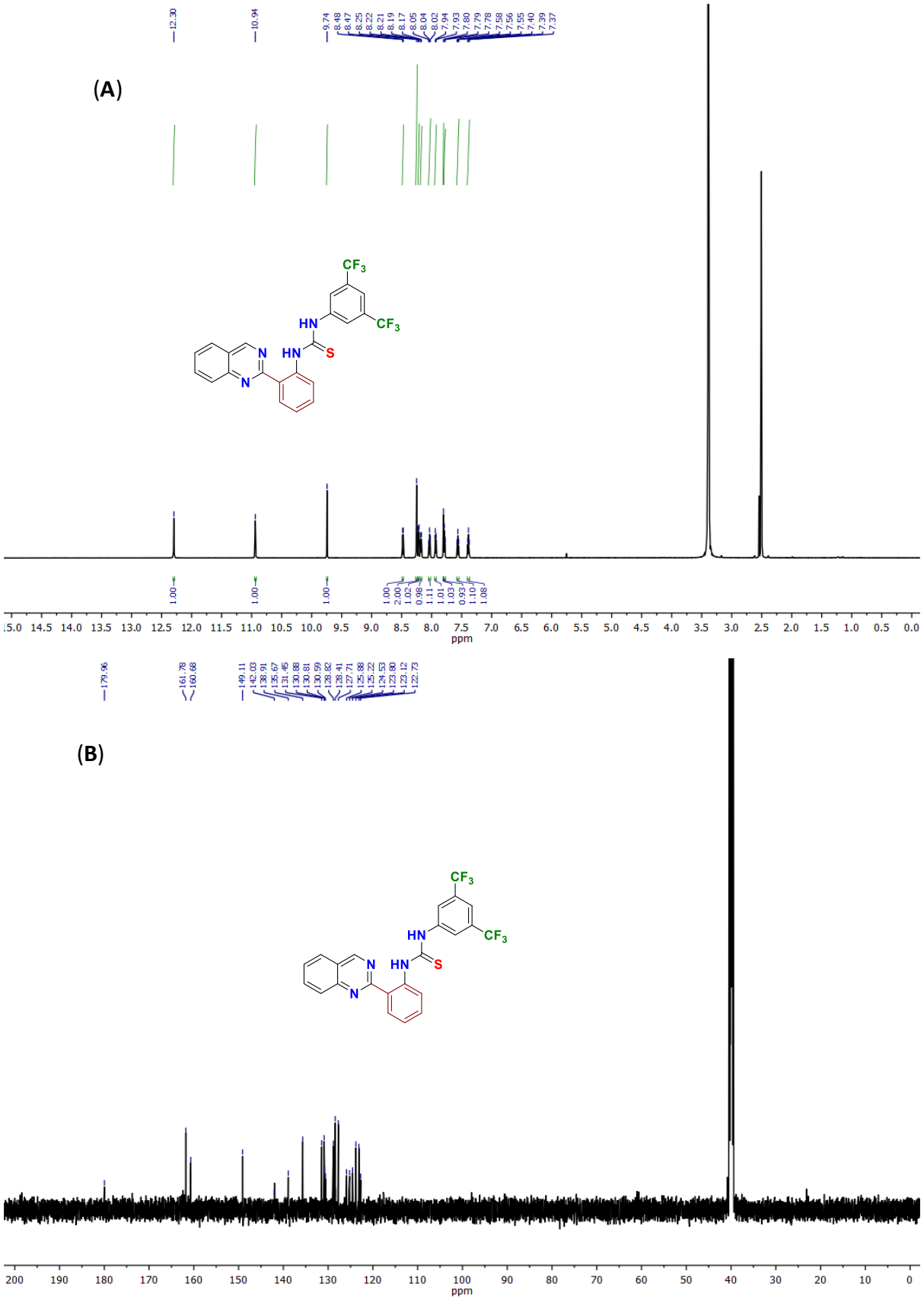

Figure S41. ^{1}H and ^{13}C NMR spectrum of compound **4** in DMSO-d_6 solvent.

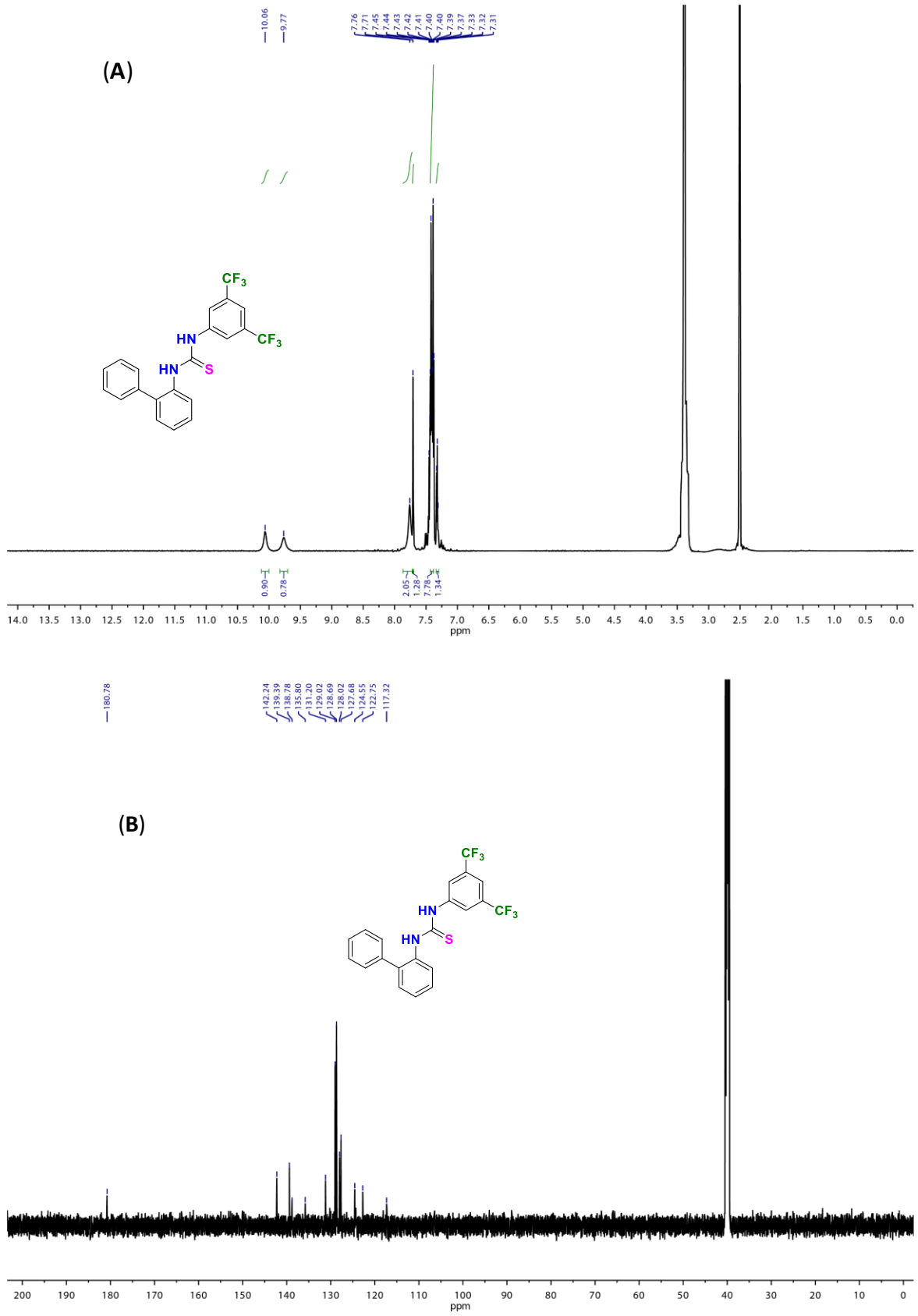

Figure S42. ^{1}H and ^{13}C NMR spectrum of compound **5** in DMSO-d_6 solvent.

11. HRMS analysis of synthesized compounds:

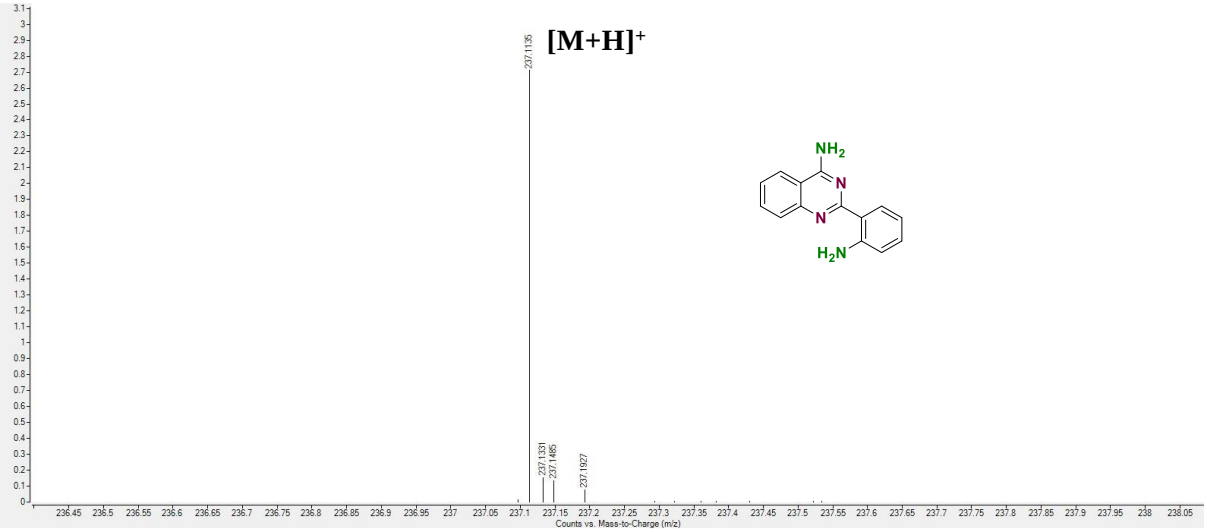

Figure S43. HRMS of 2-(2-aminophenyl)quinazolin-4-amine.

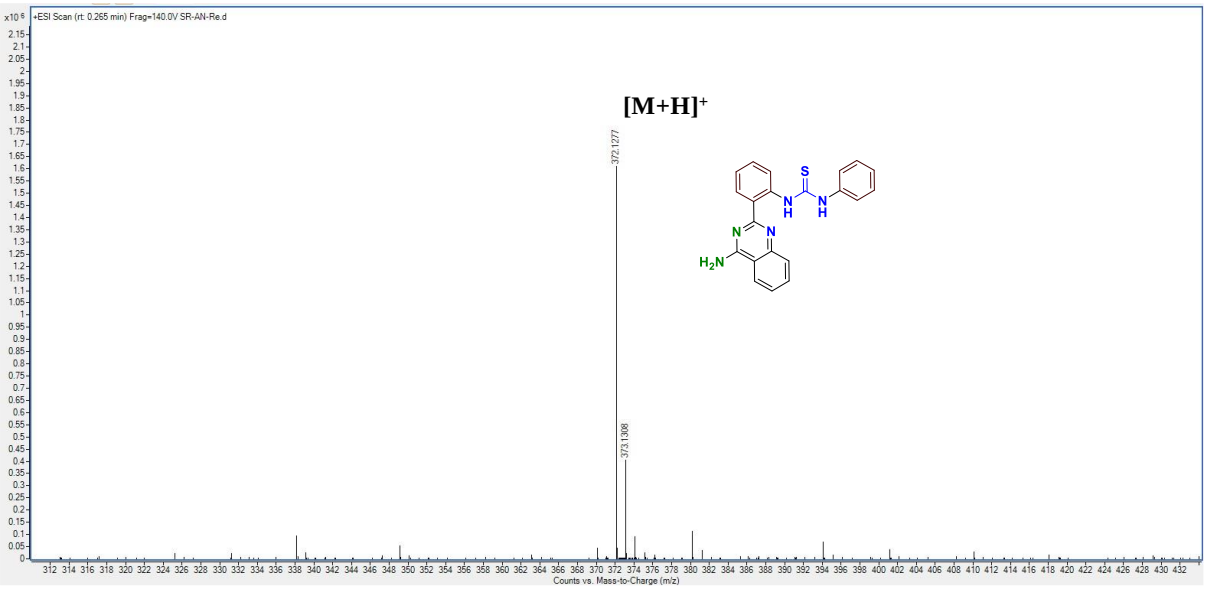

Figure S44. HRMS of **1a.**

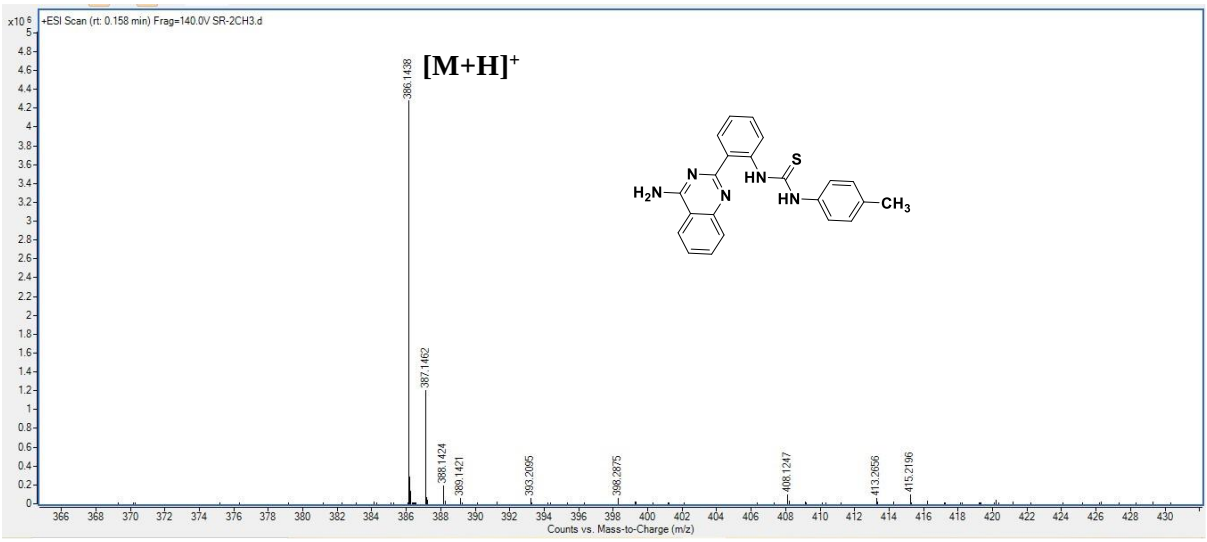

Figure S45. HRMS of **1b.**

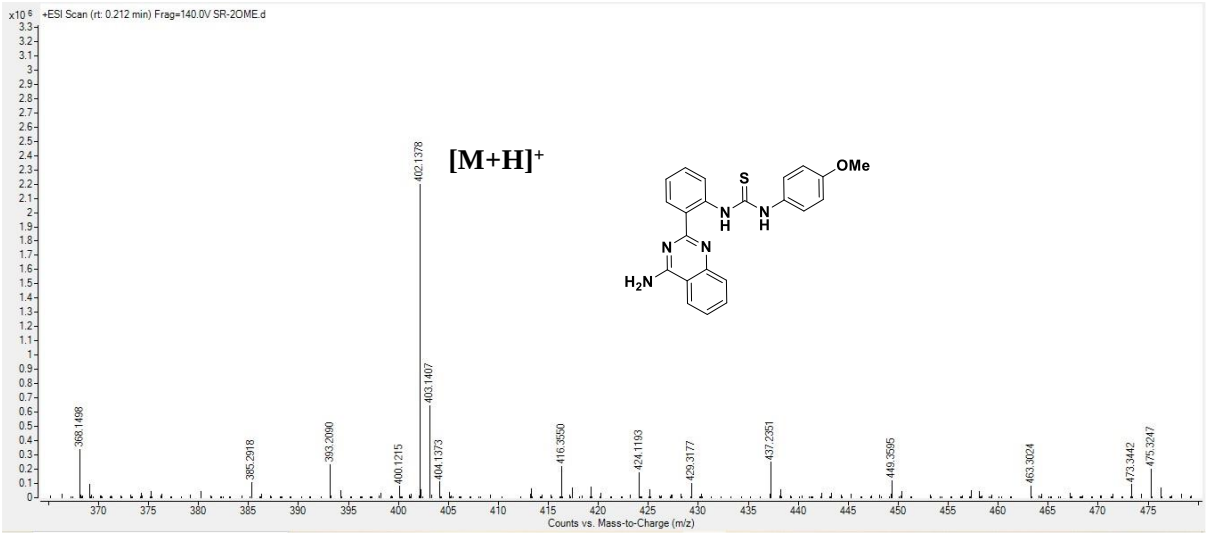

Figure S46. HRMS of **1c.**

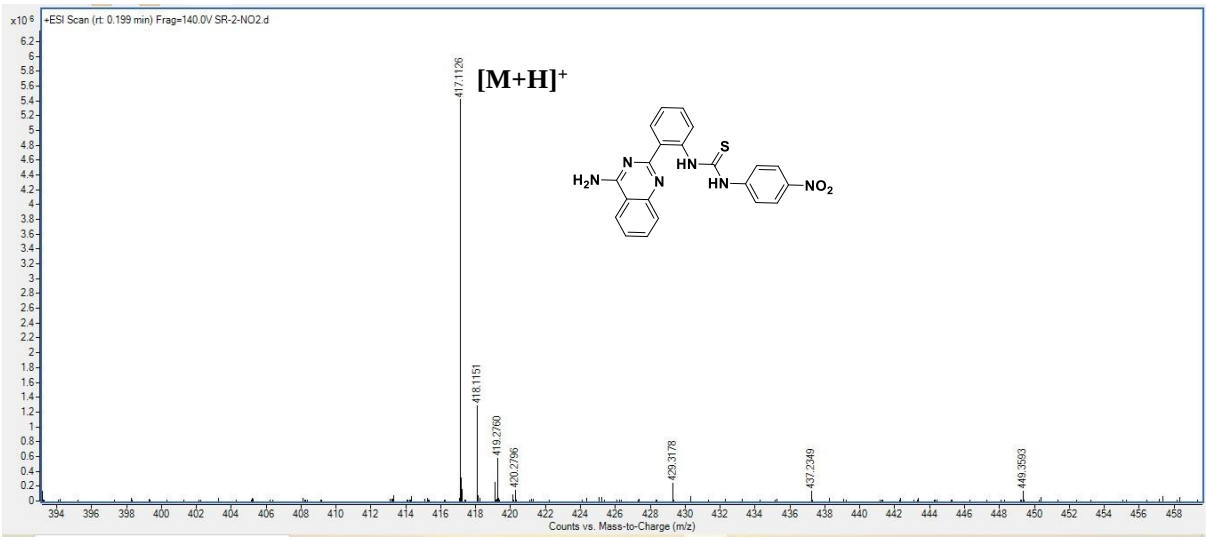

Figure S47. HRMS of **1d.**

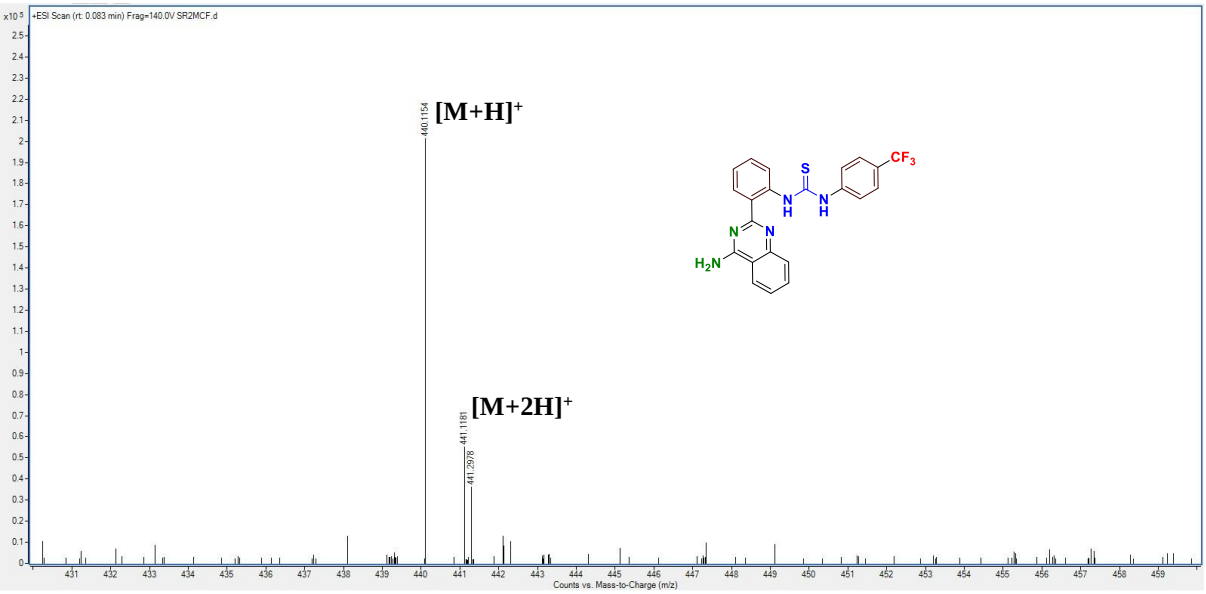

Figure S48. HRMS of **1e.**

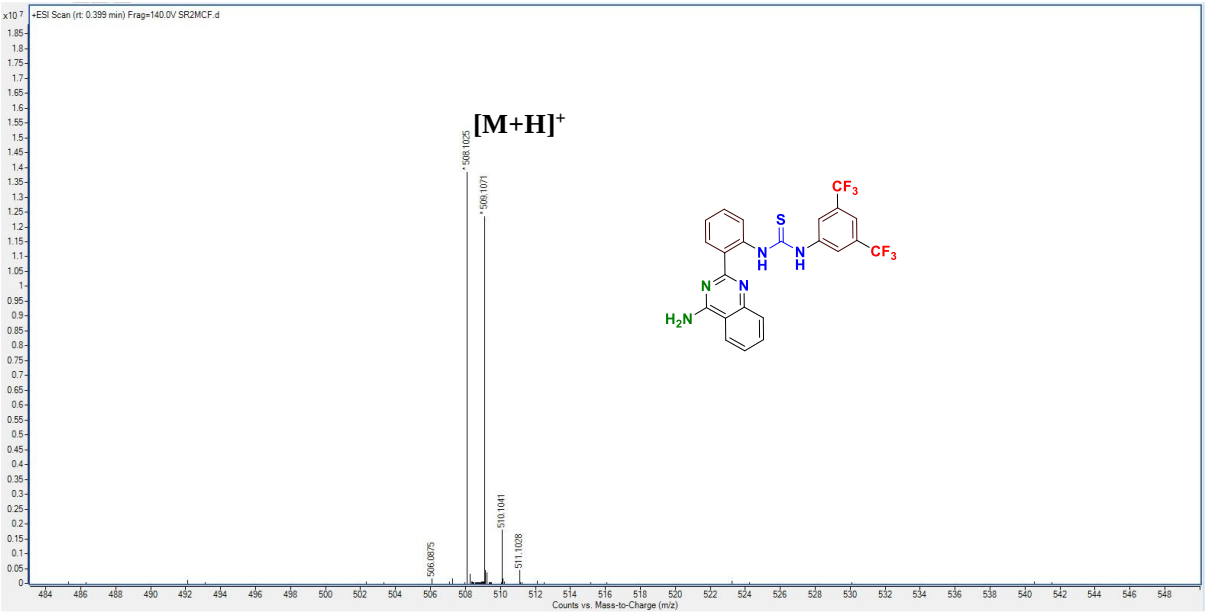

Figure S49. HRMS of **1f.**

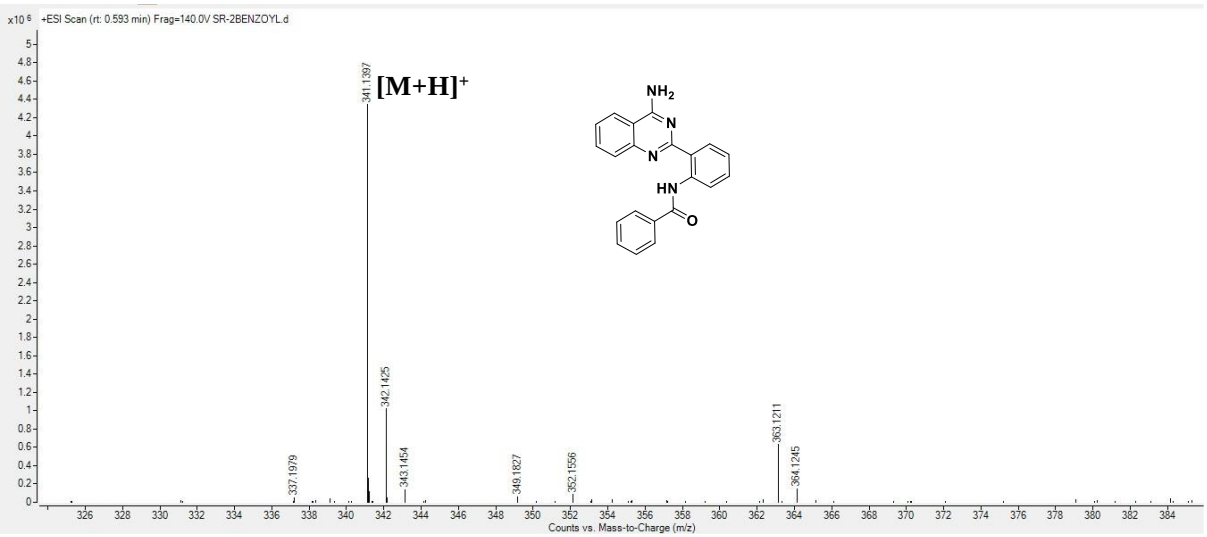

Figure S50. HRMS of **2a.**

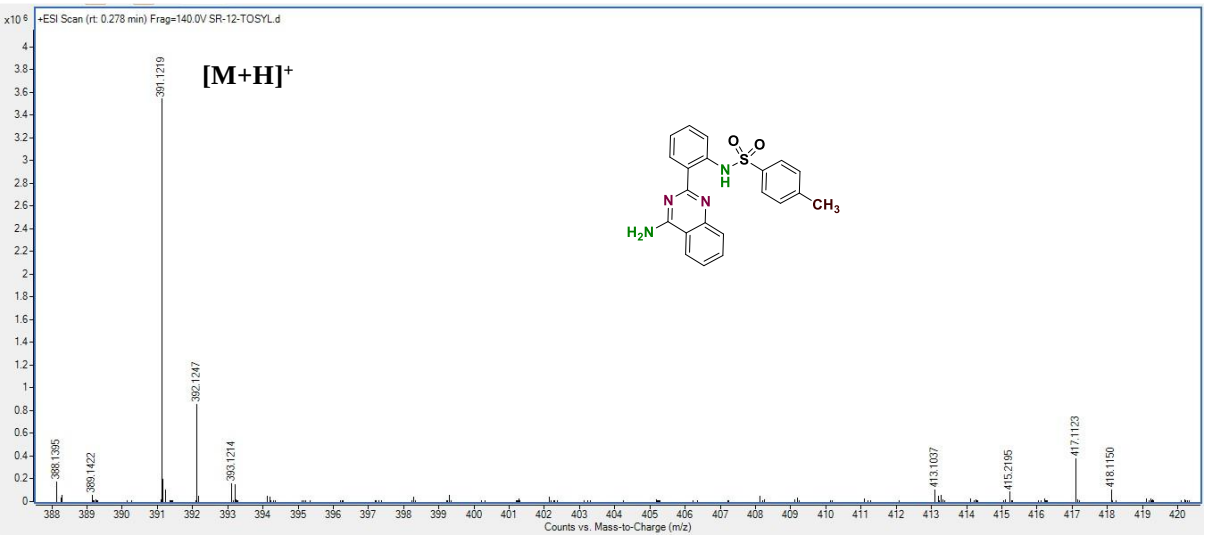

Figure S51. HRMS of **2b.**

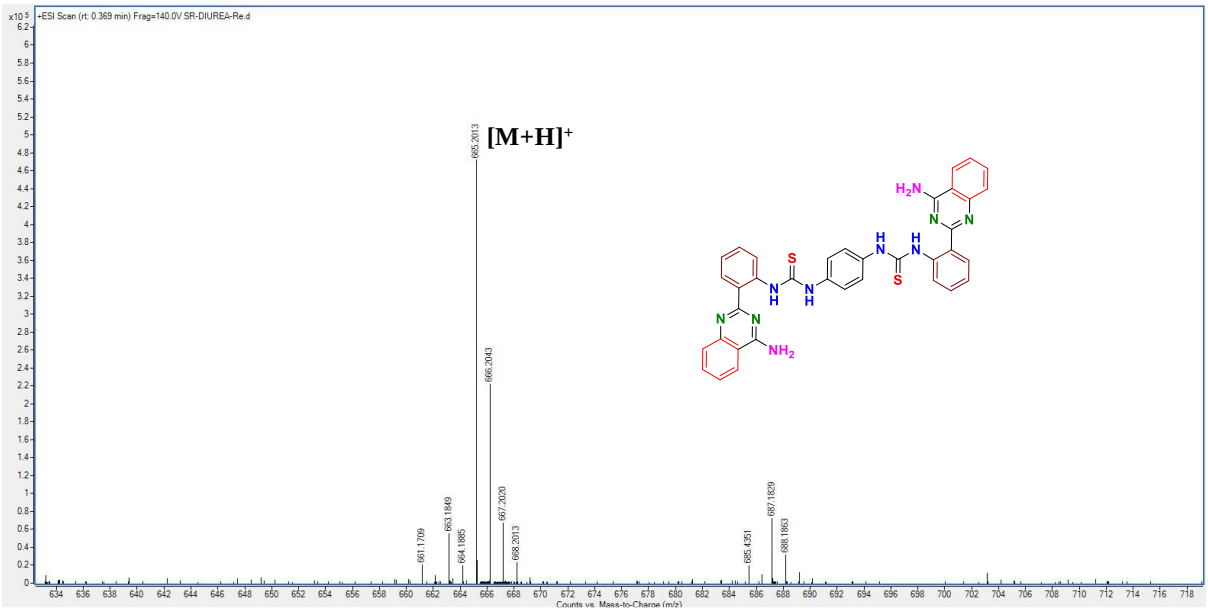

Figure S52. HRMS of **3a.**

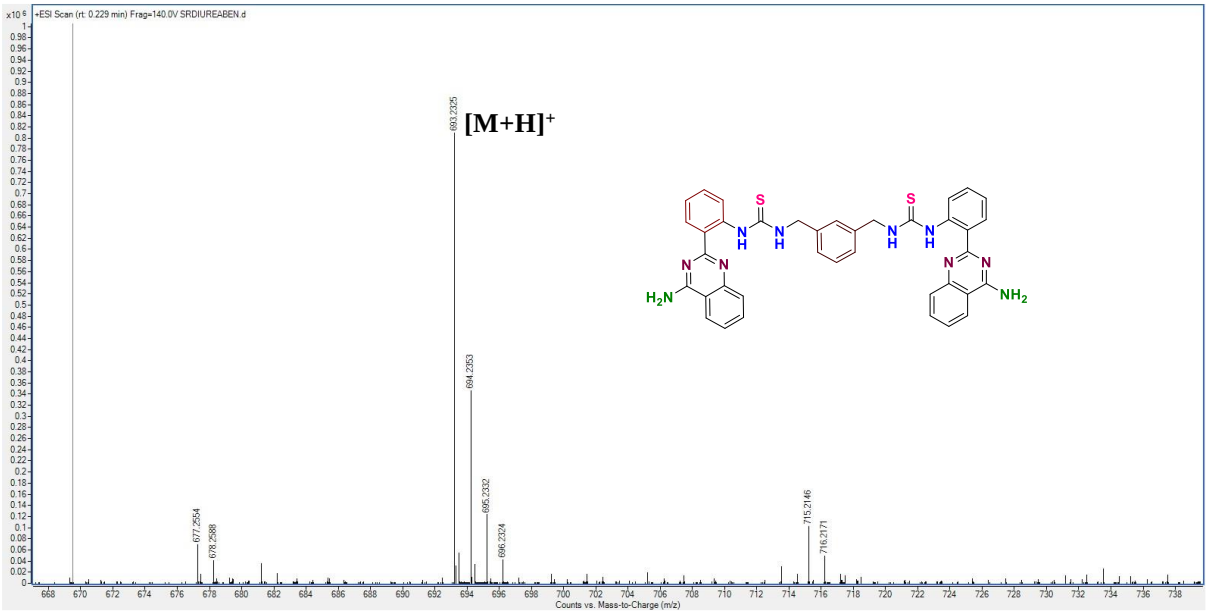

Figure S53. HRMS of **3b.**

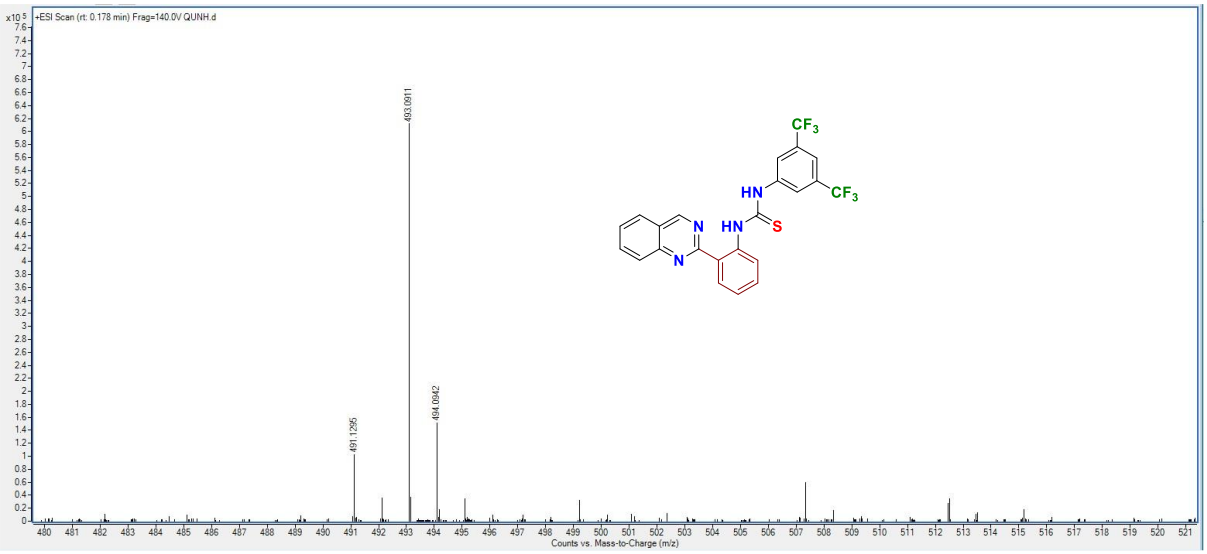

Figure S54. HRMS of compound **4.**

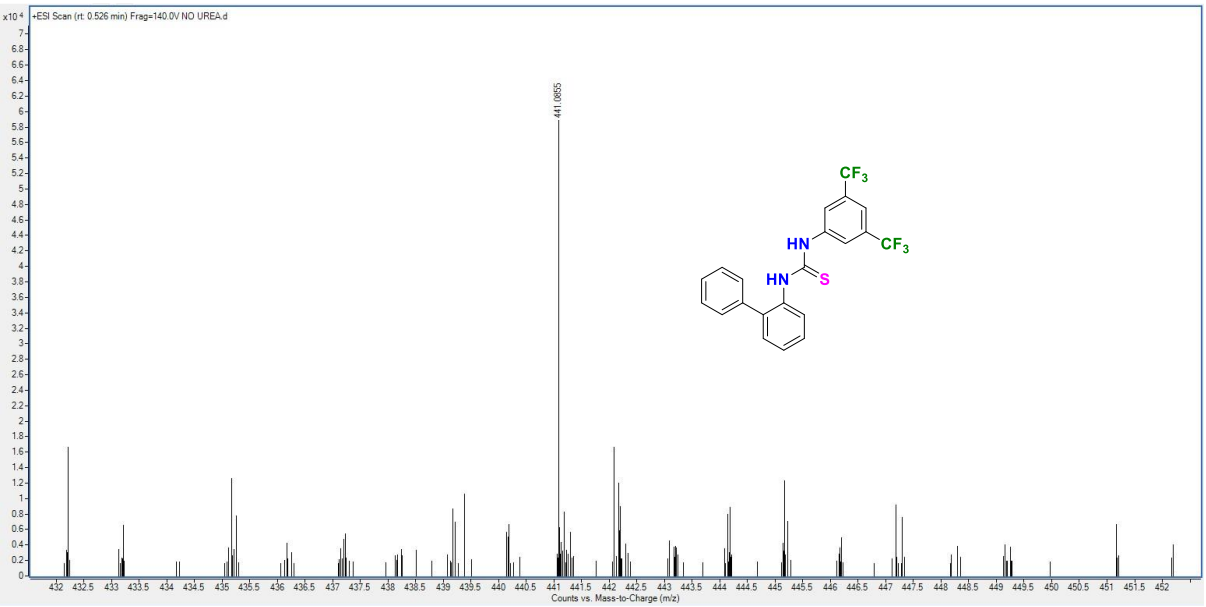

Figure S55. HRMS of compound **5**.

12. References:

1. J. E. van Muijlwijk-Koezen, H. Timmerman, H. van der Goot, W. M. P. B. Menge, J. F. V. Kunzel, M. de Groote and A. P. IJzerman, *J. Med. Chem.*, 2000, **43**, 2227-2238.
2. N. Akhtar, N. Pradhan, G. K. Barik, S. Chatterjee, S. Ghosh, A. Saha, P. Satpati, A. Bhattacharyya, M. K. Santra and D. Manna, *Acs Appl Mater Inter*, 2020, **12**, 25521-25533.
3. A. Mondal, S. N. Save, S. Sarkar, D. Mondal, J. Mondal, S. Sharma and P. Talukdar, *J. Am. Chem. Soc.*, 2023, **145**, 9737-9745.